NIH Public Access
Author Manuscript
Exp Neurol. Author manuscript; available in PMC 2014 September 01.

Published in final edited form as:
Exp Neurol. 2013 September ; 247: 143–157. doi:10.1016/j.expneurol.2013.02.012.

Comparison of sensory neuron growth cone and filopodial responses to structurally diverse aggrecan variants, *in vitro*

Justin A. Beller[a], **Brandon Kulengowski**[a], **Edward M. Kobraei**[a], **Gabrielle Curinga**[b], **Christopher M. Calulot**[a], **Azita Bahrami**[a], **Thomas M. Hering**[a], and **Diane M. Snow**[a,*]

[a]Spinal Cord and Brain Injury Research Center, and Department of Anatomy and Neurobiology, University of Kentucky, Lexington, KY 40536

[b]Seattle Children's Research Institute, Seattle, WA 98101

Abstract

Following spinal cord injury, a regenerating neurite encounters a glial scar enriched in chondroitin sulfate proteoglycans (CSPGs), which presents a major barrier. There are two points at which a neurite makes contact with glial scar CSPGs: initially, filopodia surrounding the growth cone extend and make contact with CSPGs, then the peripheral domain of the entire growth cone makes CSPG contact. Aggrecan is a CSPG commonly used to model the effect CSPGs have on elongating or regenerating neurites. In this study, we investigated filopodial and growth cone responses to contact with structurally diverse aggrecan variants using the common stripe assay. Using time-lapse imaging with 15-sec intervals, we measured growth cone area, growth cone width, growth cone length, filopodia number, total filopodia length, and the length of the longest filopodia following contact with aggrecan. Responses were measured after both filopodia and growth cone contact with five different preparations of aggrecan: two forms of aggrecan derived from bovine articular cartilage (purified and prepared using different techniques), recombinant aggrecan lacking chondroitin sulfate side chains (produced in CHO-745 cells) and two additional recombinant aggrecan preparations with varying lengths of chondroitin sulfate side chains (produced in CHO-K1 and COS-7 cells). Responses in filopodia and growth cone behavior differed between the structurally diverse aggrecan variants. Mutant CHO-745 aggrecan (lacking chondroitin sulfate chains) permitted extensive growth across the PG stripe. Filopodia contact with the CHO-745 aggrecan caused a significant increase in growth cone width and filopodia length (112.7% ± 4.9 and 150.9% ± 7.2 respectively, $p<0.05$), and subsequently upon growth cone contact, growth cone width remained elevated along with a reduction in filopodia number (121.9% ± 4.2; 72.39% ± 6.4, $p<0.05$). COS-7 derived aggrecan inhibited neurite outgrowth following growth cone contact. Filopodia contact produced an increase in growth cone area and width (126.5% ± 8.1; 150.3% ± 13.31, $p<0.001$), while these parameters returned to baseline upon growth cone contact, a reduction in filopodia number and length was observed (73.94% ± 5.8, 75.3% ± 6.2, $p<0.05$). CHO-K1 derived aggrecan inhibited neurite outgrowth following filopodia contact, and caused an increase in growth cone area and length (157.6% ± 6.2; 117.0% ± 2.8, $p<0.001$). Interestingly, the two bovine articular cartilage aggrecan preparations differed in their

© 2012 Elsevier Inc. All rights reserved

[*]*Author to whom correspondence should be addressed:* **Diane M. Snow, PhD** Professor and Endowed Chair - Spinal Cord and Brain Injury Research Center, and Department of Anatomy and Neurobiology The University of Kentucky 741 S. Limestone St. Biomedical and Biological Sciences Research Building – B455 Lexington, KY 40536-0509 Phone: (859) 323 8168 FAX: (859) 257-5737 dsnow@uky.edu.

Publisher's Disclaimer: This is a PDF file of an unedited manuscript that has been accepted for publication. As a service to our customers we are providing this early version of the manuscript. The manuscript will undergo copyediting, typesetting, and review of the resulting proof before it is published in its final citable form. Please note that during the production process errors may be discovered which could affect the content, and all legal disclaimers that apply to the journal pertain.

NIH-PA Author Manuscript
NIH-PA Author Manuscript
NIH-PA Author Manuscript

NIH-PA Author Manuscript

NIH-PA Author Manuscript

NIH-PA Author Manuscript

effects on neurite outgrowth. The proprietary aggrecan (BA I, Sigma-Aldrich) inhibited neurites at the point of growth cone contact, while our chemically purified aggrecan (BA II) inhibited neurite outgrowth at the point of filopodia contact. BA I caused a reduction in growth cone width following filopodia contact (91.7% ± 2.5, $p<0.05$). Upon growth cone contact, there was a further reduction in growth cone width and area, (66.4% ± 2.2; 75.6% ± 2.9; $p<0.05$) as well as reductions in filopodia number, total length, and max length (75.9% ± 5.7, $p<0.05$; 68.8% ± 6.0; 69.6% ± 3.5, $p<0.001$). Upon filopodia contact, BA II caused a significant increase in growth cone area, and reductions in filopodia number and total filopodia length (115.9% ± 5.4,$p<0.05$; 72.5% ± 2.7; 77.7% ± 3.2, $p<0.001$). In addition, filopodia contact with BA I caused a significant reduction in growth cone velocity (38.6 nm/sec ± 1.3 before contact, 17.1 nm/sec ± 3.6 after contact). These data showed that neuron morphology and behavior are differentially dependent upon aggrecan structure. Furthermore, the behavioral changes associated with the approaching growth cone may be predictive of inhibition or growth.

Keywords

neuronal growth cones; dorsal root ganglia neurons; velocity; extracellular matrix (ECM); regeneration; cell culture

Introduction

CSPGs are abundant in the injured spinal cord and prevent neuronal regeneration

The expression of **chondroitin sulfate proteoglycans (CSPGs)** is temporally and spatially restricted in the central nervous system (CNS) during development, and serves to guide neurons to appropriate targets, in part, by inhibiting them from entering inappropriate territories (Reichardt and Prokop, 2011, Snow, et al., 1990). Following injury to the mature CNS, the significant increase in protein levels of CSPGs surrounding the lesion (Asher, et al., 1998, Davies, et al., 1997, McKeon, et al., 1999, Oohira, et al., 1994), inhibit axonal regeneration and deter functional reconnectivity of damaged axons (Fitch and Silver, 1997, Jones, et al., 2003, Lemons, et al., 1999, Moon, et al., 2002, Pasterkamp, et al., 2001, Plant, et al., 2001, Stichel, et al., 1999). CSPGs are produced, in part, by reactive astrocytes surrounding the glial scar (Asher, et al., 2000, Fitch and Silver, 1997, Smith and Strunz, 2005). Although not without benefit to the organism, such as cordoning off the injury site, repairing the blood-brain barrier, regulating the immune response (Faulkner, et al., 2004, Myer, et al., 2006, Ribotta, et al., 2004), and limiting cellular degeneration, i.e. glutamate uptake (Beller, et al., 2011), portions of the glial scar impede neurite outgrowth and interfere with successful plasticity and regeneration (Silver and Miller, 2004). When reactive astrocytes are isolated and pretreated with chondroitinase ABC (to enzymatically remove chondroitin sulfate chains), neurite growth is increased to that observed in the presence of non-reactive astrocytes (McKeon, et al., 1995). Other studies targeting CSPG carbohydrate chains *in vivo* confirm the inhibitory activity of the carbohydrate chains on regeneration (Bradbury, et al., 2002, Galtrey, et al., 2007, Garcia-Alias, et al., 2009). Thus, CSPGs expressed by astrocytes of the glial scar, specifically the carbohydrate portion of the molecules, dramatically inhibit axonal outgrowth.

CSPG interaction with neurites is complex and involves receptor-mediated mechanisms

The neural response to inhibitory CSPGs and other CNS components involves the motile activity of the distal-most portion of a migrating or regenerating nerve cell, called the *growth cone* (Gordon-Weeks, 1989, Letourneau, 1975, Ramon y Cajal, 1928). Growth cones extend fine processes called filopodia that exert tension at points of contact and allow for adherence to other cells or surfaces. In addition to providing adhesion to support neurite

NIH-PA Author Manuscript

NIH-PA Author Manuscript

NIH-PA Author Manuscript

elongation, filopodia and growth cones interact with the extracellular matrix, through integrins and other receptors, to navigate the growing neurite towards the appropriate synaptic target(s) (McKerracher, et al., 1996, Schmidt, et al., 1995). Filopodia and growth cone interactions with the environment are highly complex and involve both adhesive and anti-adhesive functions, such as attraction and repulsion (Song, et al., 1998). The cell surface molecules that mediate cell-cell and cell-matrix interactions, modulate and are modulated by the same cytoplasmic second messenger pathways (e.g. cytoplasmic calcium signaling, protein kinases, inositol phosphates) as hormones, growth factors, neurotransmitters, and pharmaceuticals commonly target (Chierzi, et al., 2005, Giuseppetti, et al., 1994, Ivins, et al., 2004, Juliano and Haskill, 1993, Simmons, et al., 2003). Further, growth cones take on specific, pathologic morphologies when injured, as was first described by Ramon y Cajal and called `sterile clubs' or `dystrophic growth cones', and further defined by others (Horn, et al., 2008, Ramon y Cajal, 1928, Tom, et al., 2004). Thus, it is particularly relevant to examine growth cone morphologies and behaviors, as well as the molecules with which growth cones interact, to learn about putative mechanisms underlying both normal and pathological responses.

CSPGs are a complex and diverse family of proteins

Given the vast degree of diversity in CSPG structure, the resulting behavior of growth cones that contact them is likely to depend on the specific structural components of a given CSPG type. The CSPGs commonly expressed in the CNS are neurocan, brevican, versican and aggrecan, which are grouped together as lecticans, or hyalecticans (Zimmermann and Dours-Zimmermann, 2008). They have similar N-terminal hyaluronan binding domains (G1) and C-terminal globular domains (G3) that share homology to lectins. NG2 and phosphacan, two other CNS CSPGs, have structures distinct from the lecticans/hyalecticans. NG2 is a transmembrane CSPG (Lorber, 2006, Nishiyama, et al., 1991), and phosphacan (DSD-1 PG) (Maurel, et al., 1994) is a secreted splice variant of a larger transmembrane protein, RTPTß (Klausmeyer, et al., 2007). Proteoglycans can be substituted with chondroitin sulfate, dermatan sulfate, heparan sulfate, and keratan sulfate side chains (glycosaminoglycans; GAGs) in different combinations. Each carbohydrate can be sulfated in unique patterns, which imbue them with functionality (Brown, et al., 2012, Coles, et al., 2011, Laabs, et al., 2007, Wang, et al., 2008). Additionally, their core proteins may be glycosylated with N- and O-linked oligosaccharides, all providing the potential for a high level of structural diversity. The effect of each of these substitutions on neurite outgrowth is unclear, since separate conflicting data *in vitro* show that either promotion or inhibition of axonal outgrowth by CSPGs may be a result of interactions with GAG chains, core proteins, or both (Iijima, et al., 1991, Snow, et al., 1990, Snow, et al., 2001, Garwood et al., 1999). This provides yet another structural factor to address when attempting to dissect the key elements of growth cone-CSPG interactions.

Assessment of structurally diverse CSPGs effect on growth cone morphology and behavior

Aggrecan is commonly tested to explore the effects of CSPGs on neurite outgrowth, regeneration, and physiology. However, the wide structural diversity within this molecule may be critical for neuronal behavior and regeneration. Thus, in this study, we tested five different variants of aggrecan. The structures of these variants have been previously determined through biochemical analyses (Esko, et al., 1985, Miwa, et al., 2009, Miwa, et al., 2006a). Two of these variants were extracted from bovine articular cartilage, but differed in the chemical means of purification, resulting in compositional dissimilarities. We evaluated both a proprietary preparation purified through anion-exchange chromatography (Sigma-Aldrich; BA I) and a preparation produced by our laboratory using a method, which relies on hyaluronic acid binding (A1A1D1; BA II). The BA I preparation contained a

NIH-PA Author Manuscript

NIH-PA Author Manuscript

NIH-PA Author Manuscript

greater amount of fragments with cleavage products from both the N and C-terminus of the aggrecan core protein, as the negative charge of the associated chondroitin sulfate chains were used for purification. In contrast, BA II was purified using a method, which relied on hyaluronic acid binding ensuring that all purified aggrecan contained the G1 domain. In addition, three variants of recombinant aggrecan were also used, one lacking chondroitin sulfate side chains, and two with a varying number and length of chondroitin sulfate chains (Figure 1). We hypothesized these structurally diverse aggrecan variants would differentially affect the morphology and behavior of outgrowing neurites.

We used a routine outgrowth assay (stripe, or “choice” assay) combined with a novel methodology to examine overt and subtle behavioral changes in growth cones, as they made their first contact with structurally diverse aggrecan molecules *in vitro*. To model the action of regenerating growth cones that contact glial scar aggrecan following SCI, analyses were designed to compare properties of the growth cone before and after filopodial and growth cone contact with aggrecan. Thus, the assay presented in this report is a model of regenerating neurons' first contact with glial scar-relevant CSPGs.

Using time-lapse video-microscopy, chick embryonic dorsal root ganglion (DRG) growth cone properties such as general morphology, growth cone area, growth cone width and length, filopodia number and length (individually and total per growth cone), angle of approach to an aggrecan-adsorbed stripe, axonal vector, and growth cone velocity were measured. Each characteristic was compared before and after first filopodial contact and subsequent growth cone contact with aggrecan. This novel data revealed significant and rapid changes in sensory growth cone morphology and behavior resulting from filopodia and growth cone contact with substratum-bound aggrecan. These results represent potential cellular targets to clearly identify the steps necessary for successful axonal regeneration following SCI, and a useful model to test the effects of potential therapeutics on growth cone morphology of regenerating neurons.

Methods

Preparation of Structurally Diverse Aggrecan Variants

Five variants of the chondroitin sulfate proteoglycan (CSPG), aggrecan, were used in the current study to determine the response(s) of sensory neuron filopodia and growth cones to specific microstructures of aggrecan. Below is a description of the preparation of each variant.

Chondroitin sulfate-deficient aggrecan (CHO-745)—Chondroitin sulfate-deficient aggrecan (CHO-745) was prepared as described previously (Esko, et al., 1985, Miwa, et al., 2006b). Briefly, CHO(pgsA745) cells (abbreviated as CHO-745 in this paper), deficient in expression of xylosyl transferase (the enzyme that initiates chondroitin sulfate synthesis) were transiently transfected with a recombinant bovine aggrecan expression vector (pBAGG771-28) using lipofectamine 2000 (Invitrogen, Grand Island, NY). Following transfection (48 hrs), the conditioned media was collected and guanidine was added to a concentration of 4M, to ensure solubilization and denaturing of proteins. The media samples were then passed through a G-50 Sephadex (Sigma-Aldrich, St. Louis, MO) column and exchanged into a urea buffer (8 M Urea, 50mM Na-acetate, 150mM NaCl, 0.5% CHAPS, pH 6.0). Following G-50 chromatography, aggrecan was then purified through diethylaminoethyl (DEAE; Sigma-Aldrich, St. Louis, MO) anion-exchange chromatography, eluting the aggrecan with two concentrations of NaCl (250mM and 1M). The presence and concentration of aggrecan was determined through dot blot analysis.

NIH-PA Author Manuscript

NIH-PA Author Manuscript

NIH-PA Author Manuscript

CHO-K1 and COS-7 recombinant aggrecan molecules—CHO-K1 and COS-7 cells were transiently transfected with a recombinant bovine aggrecan expression vector (pBAGG71-28) using lipofectamine 2000 (Invitrogen, Grand Island, NY), as previously described (Miwa, et al., 2006b, Miwa, et al., 2009). Secreted recombinant aggrecan was purified from the conditioned medium as described above for the CHO-745 derived aggrecan variant.

Bovine Articular Cartilage derived Aggrecan (BA I)—Aggrecan BA I preparation was purchased from Sigma-Aldrich (Product # A1960; St. Louis, MO). As described in the product information sheet, BA I was extracted from mature steer articular cartilage with guanidine hydrochloride and purified using gel-filtration and ion-exchange chromatography.

Bovine Articular Cartilage derived Aggrecan (BA II)—Like BA I, aggrecan BA II was isolated from mature steer articular cartilage, but using a different technique, which produces a different compositional preparation (Miwa, et al., 2006a). Briefly, articular cartilage from 1–2 year old steer was isolated from metacarpalphalangeal joint surfaces. Proteoglycans were solubilized in ice-cold buffer (4M guanidine-HCL, 150mM sodium acetate, 50mM EDTA, pH 6.3, with protease inhibitors). The cartilage was extracted at 4°C for 48 hrs, filtered and subsequently dialyzed at 4°C for 16 hrs in 20 volumes of associative buffer (150mM sodium acetate, 5mM EDTA, pH 6.3 with protease inhibitors). BA II was then purified from solution through three separate equilibrium density gradient centrifugal separations. Specifically, the first separation was carried out under associative conditions; articular cartilage sample was placed in a 2.5M CsCl solution and centrifuged for 48 hrs at 4°C at 40,000rpm. The gradient resolved into three equal fractions called A1–A3, according to previous characterization. Fraction A1 (bottom 1/3 of associative gradient) was isolated and two volumes of disassociative buffer (5.5M guanidine HCl, 5mM EDTA, 150mM sodium acetate, pH 6.3, with protease inhibitors) were added. The solution was stirred for 4 hrs and subsequently dialyzed overnight against 20 volumes of associative buffer. The second separation in associative buffer was performed in 3.5M CsCl at 4°C for 48 hours at 40,000rpm. The resulting bottom third of the sample (Fraction A1A1) was subjected to a final equilibrium gradient centrifugal separation under dissociative conditions. The gradient resolved into three equal fractions, called D1–D3, and fraction D1 was dialyzed against 100mM sodium acetate/5mM EDTA, 50mM sodium acetate/2.5mM EDTA, followed by three changes of water. The sample was lyophilized and stored at −80°C. The aggrecan preparation used was the fraction A1A1D1.

Neurite Outgrowth Stripe Assay

Substratum Preparation—This laboratory and many others have historically used a patterned substratum to introduce molecules of interest into the path of elongating axons (Letourneau, 1975, Snow, et al., 2001). In this study, we chose a basic paradigm of adsorbing aggrecan and laminin in a striped pattern with modifications to improve optical resolution (Snow et al., 2001). Briefly, glass coverslips were mounted over 22 mm holes in the bottom of 50 mm polystyrene Petri dishes. A 0.1 mg/ml poly-D-lysine solution (in borate buffer; 50mM Boric Acid, 24mM sodium tetraborate decahydrate) was applied to the coverslip (2 hrs; room temperature (RT)) to provide an adhesive substratum for the binding of the aggrecan variants to glass. The coverslips were washed (2×) with PBS and air-dried at RT for 1 hr. Each aggrecan variant (150 μg/ml) was mixed with Alexa 555 fluorochrome (to identify the region where aggrecan was bound; Invitrogen; Grand Island, NY) and applied by soaking cellulose strips (1 cm × 250 μm; cut from Whatman filter paper) in the aggrecan mixture and placing the strips on the poly-D-lysine coated glass coverslip until dry (5 minutes). Once the aggrecan was transferred to the substratum and the cellulose strips were removed, laminin (25 μg/ml) was applied to the entire coverslip, and incubated at RT for 1

NIH-PA Author Manuscript

NIH-PA Author Manuscript

NIH-PA Author Manuscript

hr with gentle agitation. The surface of the coverslip was washed to remove unbound aggrecan and laminin. The result was a patterned substratum consisting of alternating stripes of aggrecan + laminin, and laminin alone (Figure 2A). This method was performed using each of the aggrecan variants mentioned above.

Sensory Neuron Dissection—Embryonic dorsal root ganglia (DRG; E9–12; chicken) neurons were dissected according to AAALAC regulations (UK IACUC protocol #0086M2005) and transferred to culture dishes containing 500 μl of serum-free Dulbecco's Modified Eagle Media (DMEM) with F12 in a 1:1 ratio; supplemented with 0.5% bovine serum albumin, 25mM HEPES, 5mM phosphocreatine, 1mM sodium pyruvate, 50 ng/mL NGF (R&D Systems; Minneapolis, MN), and N2 supplement (Invitrogen; Grand Island, NY). The DRG were cut into small explants and plated on the substratum described above (Figure 2A). The tissue culture plates were incubated at 37°C for approximately 16 hrs.

Growth Cone Morphology Measurements

A wide variety of filopodial and growth cone morphologies and behaviors were examined in detail to determine the overt and subtle response to the above aggrecan variants. This section describes each analysis.

Image Acquisition—In order to ensure that first contact of a filopodia with the aggrecan-adsorbed stripe was captured, we conducted a pilot study. Growth cones were imaged at 1 frame per second. From this pilot study, we determined that an interval of 15 sec was sufficient to observe all critical filopodia behaviors, including first contact with the aggrecan-adsorbed stripe. For all subsequent experimentation, we imaged the outgrowing neurites at a rate of 15 sec/frame. A Zeiss Axiovert 200M with a 40× air objective was used. Both a phase-contrast and Texas Red epifluorescent image was captured of each frame, displaying the neurite and aggrecan-adsorbed stripe respectively. These images were then analyzed using the methods described below.

Growth Cone Root identification: To dependently measure changes in growth cone morphology, it was necessary to identify the growth cone root. For neurons with stereotypical, large, “hand-like” growth cones, the identification of the “root” of the growth cone, i.e. the demarcation between growth cone and axon, was obvious. However, in many cases, normal growth cones take on a narrow, or “bullet-shaped” morphology, and the location of the root is no longer clear. For this reason, we analyzed 100 stereotypical (hand-shaped) growth cones from 3 experiments, and measured the distance between the tip of the leading edge of the growth cone (not including filopodia) and the obvious root. From these experiments we determined that the average distance was 10 μm. For all subsequent experiments, we used this average distance (10 μm) from tip to root to demarcate the growth cone root in all growth cones with an unidentified root. While this has inherent error, using the same procedure for all growth cones over hundreds of measurements provided a reasonable means for comparison between growth cones under differing conditions.

Measurement #1. Growth cone length and width: Growth cone length and width were measured at the widest points for each. The Zeiss *Rectangle Tool* (Zeiss, Inc., Axiovision 4.4) was extended until all four sides just touched the maximum extension of the growth cone in each direction, matching the axon-facing side at the growth cone root (see “Growth Cone Root” above). The rectangle formed was perpendicular to the growth cone vector. The rectangle distance parallel to the vector was recorded as the length (μm). The rectangle distance perpendicular to the vector was recorded as the width (μm).

NIH-PA Author Manuscript

NIH-PA Author Manuscript

NIH-PA Author Manuscript

Measurement #2. Growth Cone Area: The point of the growth cone perimeter where a filopodia began was marked with an "X" on the growth cone image for each frame. To qualify as a filopodia, the projection had to be a rigid, linear (actin-based) projection of ≥5 μm long and 0.8–1.2 μm wide. These morphological guidelines were used to distinguish a filopodia from a lamellopodia, defined as ≥1.3 μm wide and contained within the growth cone perimeter. The *growth cone root* was also marked with an "X" (see "Growth Cone Root" above). At high magnification, the marked "X's" were connected using the "outline" tool (Zeiss, Inc., Axiovision 4.4), and the growth cone area of this boundary was automatically determined, excluding filopodia, but including lamellipodia/veils.

Measurement #3. Filopodial length: The length of each growth cone projection meeting the criteria of filopodia (see "growth cone area") was measured, beginning with the "X" along the growth cone perimeter (see "growth cone area") moving away from the body of the growth cone, using digital calipers. If the observer questioned whether an item qualified as a filopodia, he/she viewed numerous frames prior to and after the frame in question to determine if it was a filopodia or a transient projection of the growth cone membrane. Filopodia were excluded if they did not continually meet the criteria for filopodia dimensions (see "growth cone area"), for instance if they extended out of the field of view, extended under or over another structure, or folded back upon itself. All measurements were stringently conservative, requiring complete compliance with all criteria to be included in the analysis.

Measurement #4 – 5. Total Filopodia and Average Filopodia Number: All structures that met the criteria for a filopodia were counted and totaled for each growth cone. These were expressed as total number of filopodia per growth cone, and as the average number of filopodia per growth cone of a given population.

Measurement #6 – 7. Growth Cone Approach Angle and Velocity: In order to determine the angle of approach of an elongating growth cone, a vector representation of the growth cone was constructed. A line was drawn along the length of the axon, through an "X" positioned on the elongating growth cone root (see above definition), through an "X" placed at the central domain of the growth cone (visualized with phase microscopy; 40×), and onward until reaching the edge of the aggrecan stripe. A reference vector was then constructed by following the edge of the aggrecan-adsorbed stripe. The angle of approach was then measured using the "Angle" Tool (Zeiss, Inc., Axiovision 4.4), measuring the angle between the two vectors. This allowed direct measurement of the growth cone approach angle.

The velocity (distance the growth cone traveled over time) was determined over the course of 40 frames – 20 frames prior to and 20 frames after first filopodia contact. To calculate the velocity of the growth cone, the distance traveled by the growth cone root along the angle of trajectory (mentioned above) over 10 frames was measured and then divided by the amount of time (150 seconds).

Data and Statistical Analysis

Statistical analysis was performed using SPSS software (Version 20; IBM, Chicago IL). Alpha level for Type I error was set at 0.05 for rejecting the null hypothesis.

All parameters were normalized to the average calculated for Zone 1 for each individual neurite. Zone 1 values were averaged and then compared to the raw values in order to determine the SEM for the Zone 1 measurements. Zone 2 and Zone 3 measurements were then compared to the Zone 1 averages, converting the measurements into percent of Zone 1

NIH-PA Author Manuscript

NIH-PA Author Manuscript

NIH-PA Author Manuscript

values for each individual data point. These individual data points were then averaged together (by Zone) to express the mean as percent of Zone 1 levels. ANOVA analysis was conducted separately for each parameter (i.e. length, or width). Dunnett post-hoc analysis was then conducted comparing Zone 2 and Zone 3 to Zone 1 in order to determine significance. In those scenarios in which the growth cone did not reach Zone 3, standard T-tests were used to determine significance between Zone 1 and Zone 2 levels.

For the velocity studies, the velocity measured for the 20 frames prior to filopodia contact was averaged and compared to the average of the 20 frames following filopodia contact using a standard T-test.

Results

Development and verification of novel time-lapse methodology for measuring growth cone and filopodia responses

Dorsal root ganglia neurons are inhibited by substratum bound CSPGs—The inhibitory influences of CSPGs on neurite outgrowth are well documented using a wide variety of experimental paradigms and for many neuronal cell types (Kofron, et al., 2009, Li, et al., 2008, See, et al., 2010, Snow, et al., 2001, Tom, et al., 2004). However, novel to the present report, neuronal growth cones undergo rapid and significant morphological and behavioral changes; 1) merely by making CSPG contact via a *single* filopodia, and 2) that are dependent upon the structural composition of the CSPG (Figure 3).

Annotation and measurement of growth cone changes—Sensory neurons placed on a patterned substratum containing alternating regions of CSPG-laminin and laminin alone, *in vitro*, were analyzed for changes in growth cone morphology. Neuronal growth cones grew from regions adsorbed solely with laminin toward CSPG-laminin adsorbed regions, and contacted the CSPG stripe. Using numerous time-lapse microscopy image series prior to, during, and after contact, total growth cone area, growth cone width and length, filopodia number, filopodia length (individually and total per growth cone), angle of approach to CSPG stripe, growth cone vector, and growth cone velocity were measured and recorded. Figure 4 is a representative image of a typical assessment of growth cone morphology using the Axiovision image analysis system (Version 4.4, Zeiss, Inc.), performed on repeated frames during a single growth cone's elongation.

User consistency; reliability of measurement data—Examination of growth cone behaviors required detailed measurements of many growth cone traits over hundreds of time-lapse video frames. It was therefore essential to be assured that measurements by different users were consistent. Thus, a detailed protocol was constructed with multiple criteria for each type of measurement. To determine the success of this training for each user, we conducted an experiment where each user measured the same frame series (100 frames), and the results obtained by each user were compared.

In Figure 5, the left and center panels (Users A and B) show measurements of growth cone length acquired from two experienced measurers, and the right panel (User C) shows results obtained by a novice measurer following an initial training using the designed rubric. There is a great similarity between the two experienced measurers (left and center panel) and between the experienced measurers and the novice measurer (right panel). This result suggests that the use of a detailed rubric, combined with hands-on instruction, leads to consistent data among different measurers. Regardless of the notable reliability of data acquired by new measurers, data was not used until a measurer was in the “experienced” range, i.e. those having performed analysis of greater than 20 traces (e.g. User A).

NIH-PA Author Manuscript

NIH-PA Author Manuscript

NIH-PA Author Manuscript

Differential responses to structurally diverse aggrecan variants

CHO-745 derived aggrecan allowed extensive growth across the aggrecan stripe and caused numerous changes in growth cone and filopodia behavior

—CHO-745 derived aggrecan does not contain chondroitin sulfate chains due to a lack of xylosyl transferase. The CHO-745 derived aggrecan did not inhibit neurite outgrowth and allowed extensive growth across the stripe (Figure 6). Growth cone width and filopodia length were significantly increased following filopodia contact with the stripe (Zone 1 to 2), with values of 112.7% ± 4.9 and 150.9% ± 7.2 of Zone 1 values, respectively ($p<0.05$; Figure 6A, B). When the growth cone made contact with the stripe (Zone 3) there was a significant increase in growth cone width (121.9% ± 4.2, $p<0.001$), and reduction in filopodia number (72.39% ± 6.4, $p<0.05$) when compared to Zone 1 values (Figure 6A, B).

COS-7 derived aggrecan was inhibitory to neurite outgrowth and associated with changes in growth cone area, width, length, and filopodia number and length

—DRG neurons were inhibited by the presence of COS-7 derived aggrecan. Growth of the extending neurites progressed through the area of filopodia contact (Zone 2) and was inhibited at the time the growth cone made contact with the stripe (Zone 3) (Figure 7). As the outgrowing neurite's filopodia contacted the COS-7 derived aggrecan (Zone 2) there was a significant increase in growth cone area (126.5% ± 8.1, $p<0.001$) and width (150.3% ± 13.31, $p<0.001$) compared to Zone 1 values (Figure 7A). At the point the growth cone contacted the COS-7 derived aggrecan (Zone 3) both growth cone area and width returned to Zone 1 levels, however there was a significant decrease in filopodia number (73.94% ± 5.8, $p<0.05$) and length (75.3% ± 6.2, $p<0.05$) compared to Zone 1 values (Figure 7B).

CHO-K1 derived aggrecan is inhibitory to neurite outgrowth and associated with changes in growth cone area, and length

—In response to CHO-K1 derived aggrecan the growth cone retracted upon filopodia contact and did not progress into Zone 3 (Figure 8). There was a significant increase in growth cone area (157.6% ± 6.2, $p<0.001$), and length (117.0% ± 2.8, $p<0.001$) following filopodia contact compared to Zone 1 values (Figure 8A). There was no change in filopodia number, total length, and max length (Figure 8B).

Bovine aggrecan is greatly inhibitory to neurite outgrowth and causes significant changes in growth cone and filopodia behavior

—The bovine aggrecan preparations we examined in our study caused numerous changes in growth cone behavior. We examined both a commercially available preparation (Sigma, Bovine Aggrecan I; BA I) and a preparation prepared by our laboratory through the A1A1D1 methodology (Bovine Aggrecan II; BA II). Both of these preparations prevented growth of the neurite onto and across the aggrecan stripe. Through Western blot analysis BA I was determined to contain a greater amount of aggrecan fragments as compared to BA II (data not shown), as would be predicted based on the differences in preparation. BA I allowed growth up to Zone 3, while the BA II prevented the growth cone from reaching Zone 3 (Figure 9, 10). Following filopodia contact with the BA I stripe (Zone 2) there was a reduction in growth cone width (91.71% ± 2.5, $p<0.05$) and max filopodia length (90.24% ± 3.5, $p<0.05$) as compared to Zone 1 values. Growth cone contact with BA I (Zone 3) caused a significant reduction in growth cone area (75.6% ± 2.9, $p<0.05$) and width (66.4% ± 2.2, $p<0.001$) as compared to Zone 1 values (Figure 9A). In addition, BA I caused changes in filopodia behavior with reductions in filopodia number (75.9% ± 5.7, $p<0.05$), total length (68.8% ± 6.0, $p<0.001$) and max length (69.6% ± 3.5, $p<0.001$) after growth cone contact with the BA I stripe (Zone 3) (Figure 9B).

NIH-PA Author Manuscript

NIH-PA Author Manuscript

NIH-PA Author Manuscript

BA II caused a different response in DRG neurite outgrowth, but was also fully inhibitory. In response to BA II, growth cones were inhibited following filopodial contact (Zone 2) thereby preventing the growth cone from contacting the stripe (Zone 3) (Figure 10). A significant increase in growth cone area (115.9% ± 5.4, $p<0.05$) and width (118.8% ± 4.5, $p<0.05$) was observed following filopodia contact compared to Zone 1 values (Figure 10A). While a significant reduction in total filopodia number (72.5% ± 2.7, $p<0.001$) and length (77.7% ± 3.2, $p<0.001$) was observed compared to Zone 1 values (Figure 10B). The results from these analyses are summarized in Table 1.

A single filopodia contact resulted in a dramatic change in growth cone velocity—In order to measure the effect of a single filopodia touch on growth cone velocity, we analyzed 8 neurites (from 8 different animals) as they came into contact with BA I. For analysis, 20 frames before filopodia contact and 20 frames after were used (at a rate of 15 sec/frame; see *Methods*). Figure 11 shows a representative growth cone and its assessment of velocity. The left-most "X" marks the distal part of the central domain of the growth cone and the right "X" marks the growth cone root by which angle of trajectory was determined (Figure 11A). This vector was extended to intersect with the aggrecan (vertical) border, and the growth cone angle of approach was determined by comparing to a reference vector drawn parallel to the aggrecan border.

In Fig. 11B, the left-most and middle "X" in panels A and B mark the distal end of the central domain of the growth cone, and the growth cone root, respectively. The right-most "X" was the position of the growth cone root *ten frames prior to the one shown*. Therefore, measuring the distance the growth cone root moved over time yields the velocity of the growth cone. As shown in Figure 11B, a parallelogram was used to measure the distance, or the change in growth cone root position. Growth cone approach velocity was significantly decreased immediately following the *first filopodia contact* with BA I (Figure 12A) as the growth cone moved at a velocity of 38.6 nm/sec ± 1.3 before filopodia contact and slowed to 17.1 nm/sec ± 3.6 after filopodia contact (Figure 12B).

Discussion

Chondroitin sulfate proteoglycans inhibit neurite outgrowth following spinal cord injury

Chondroitin sulfate proteoglycans (CSPGs, e.g. aggrecan) are large, structurally complex extracellular matrix molecules. CSPGs are upregulated in response to nervous system injury and subsequently inhibit axonal regeneration. The neuronal growth cone is the portion of the regenerating nerve cell that makes first contact with CSPGs, therefore, we sought to model that interaction *in vitro* and to examine whether the growth cone can detect differences in variations in CSPG structure. One main goal of the study was to develop a method to intricately model the primary interactions of growing neurites when approaching a CSPG-rich glial scar that forms following injury *in vivo*. By using time-lapse video imaging and static imaging of dorsal root ganglion (DRG) sensory neurons *in vitro*, the interaction of growth cones with a variety of CSPGs was assessed. For this study, we selected chicken DRG neurons (to compare with previous studies from our lab and many others) and structurally diverse forms of the CSPG, aggrecan. Current studies are underway to repeat these assays using adult DRG neurons.

Aggrecan is the most widely studied CSPG used to model and investigate outgrowing neurites interaction with CSPGs. Although there are many CSPGs in the central nervous system (e.g. brevican, neurocan, phosphacan, versican, decorin) we desired to use aggrecan to compare to the many studies in the literature, and to utilize our expertise in producing and testing structurally diverse forms of aggrecan. The stripe assay was used in this study to subject outgrowing neurites to a steep change in CSPG concentration, reminiscent of what

NIH-PA Author Manuscript

NIH-PA Author Manuscript

NIH-PA Author Manuscript

may occur at the glial scar. Other models such as the proteoglycan spot model (Tom et al., 2004) likely mimic a different gradient in CSPG concentration, which may cause different effects on growth cone morphologies and subtle behaviors. Importantly, both paradigms result in high levels of neurite outgrowth inhibition.

Limitations of Our Approach

In this project, we used embryonic DRG neurons to investigate the effect different structural variants of aggrecan had on growth cone and filipodia behavior. Numerous studies from our laboratory and others have used embryonic neurons to measure the effect of CSPGs on neurite outgrowth (Condic, et al., 1999, Fok-Seang, et al., 1995, Hynds and Snow, 2001, Koprivica, et al., 2005, Lemons, et al., 2005, Snow, et al., 1994, Snow, et al., 1990a, Snow, et al., 2001, Snow, et al., 1990b, Yu and Bellamkonda, 2001). Thus, to compare directly the current findings with previous results from our own laboratory, as well as to those of numerous other investigators, we used embryonic neurons. Although studies using adult DRG neurons may represent a more physiologically relevant model given that the overarching goal is to understand the role CSPGs play in inhibiting regeneration of the adult injured spinal cord, there is not ample evidence suggesting the response of adult neurons to CSPGs differs from that of embryonic neurons (Busch and Silver, 2007, Fok-Seang, et al., 1995, Zhou, et al., 2006, Zuo, et al., 1998b; D. Snow, unpublished data using young adult DRG and 5-HT neurons). Both embryonic and adult neurons are inhibited by CSPGs and other proteoglycans, and within a comparable concentration range.

The structural variants we used in our study varied in the number of CS chains and types of fragments in each preparation. This makes confirming that equal concentrations of each variant were adsorbed to the plate problematic and complicated. There are a number of ways of detecting the presence of aggrecan or CSPGs in general, which include the dimethylmethylene blue (DMMB) assay, a uronic acid assay, the Alcian blue assay, and immunoreactivity. However, none of these would yield a reliable result. For instance, the DMMB, uronic acid, and Alcian blue assays all rely on a colorimetric reaction between a dye and different components of the associated GAGs (Barbosa, et al., 2003, Masuda, et al., 1994, van den Hoogen, et al., 1998). Since, our variants differed in the amount of GAGs these assays would not produce reliable measurements to determine equal concentrations of aggrecan bound to each region of the culture dish. Immunoreactivity quantification would use antibodies specific to different components of either the core protein or epitopes of the associated GAGs. Since our variants differed in both the amount of GAG and fragments present, this method would also be unable to produce reliable measurements to determine whether we had an equal presence of aggrecan bound. In addition, there is no evidence suggesting that there is a direct interaction between the amount of GAG associated with the core protein and its ability to bind to a poly-d-lysine coated substratum. Furthermore, evidence suggests that aggrecan binds to laminin via its core protein (Hynds and Snow, 2001, Snow, et al., 1996). However, the possibility that there could be a difference in the amount of bound CSPG is a reality and a limitation to our approach. While we will continue to pursue valid means by which to substantiate exact binding of each variant, it is unlikely that unequal binding is cause for such diversity in results. For example, a wide range of concentrations of intact CSPGs as well as CSPGs treated with chondroitinase, keratanses, hyaluornidase, or PNGase have been performed by our laboratory, and do not simply mirror the results seen with comparative analysis of the current, engineered CSPG variants, but rather reveal additional detail.

Inhibitory effect of aggrecan depends on the presence of chondroitin sulfate chains

Aggrecan produced by CHO-745 cells does not contain chondroitin sulfate chains due to the lack of xylosyl transferase (Miwa, et al., 2006a). Many studies show that the enzymatic

NIH-PA Author Manuscript

NIH-PA Author Manuscript

NIH-PA Author Manuscript

removal of chondroitin sulfate chains on aggrecan abolishes the inhibitory effect on outgrowing neurites *in vitro* and *in vivo* (Barritt, et al., 2006, Laabs, et al., 2007, Massey, et al., 2006, Snow, et al., 1990, Yick, et al., 2003, Zuo, et al., 1998a). In agreement with these previous studies, outgrowing neurites were not inhibited by CHO-745 derived aggrecan. Therefore, the absence of chondroitin sulfate, albeit enzymatically or genetically, abolishes the inhibitory effect of aggrecan. Studies *in vivo* demonstrate that chondroitin sulfate digestion can augment regeneration in some models, but only minimal success has been achieved to date. Thus, the removal of chondroitin sulfate is an important step in regeneration, but does not appear to be the "magic bullet".

Upon growth cone contact with an aggrecan border there is a reduction in filopodia number

CHO-K1-derived and A1A1D1-purified bovine articular cartilage aggrecan (BA II) did not permit growth cones to contact the aggrecan stripe, because the outgrowing neurite retracted following filopodia contact. In contrast, CHO-745-derived, COS-7-derived, and the proprietary bovine articular cartilage aggrecan (BA I) permitted the growth cone to make contact with the aggrecan border. In all the conditions permitting contact of the growth cone with the aggrecan stripe there was a significant reduction in filopodia number. This may implicate the role of aggrecan in not only inhibiting neurite outgrowth, but also in directing and controlling synaptic connections. Specifically, aggrecan is abundant in central nervous system extracellular structures, termed "perineuronal nets" (PNNs) (Matthews, et al., 2002, McRae, et al., 2007, Morawski, et al., 2010). These structures encapsulate neurons in the central nervous system, determine formation of synaptic connections, and prevent aberrant synaptic connections (Dityatev, et al., 2010, Frischknecht and Seidenbecher, 2008, Reimers, et al., 2007). Upon contacting aggrecan, the reduction in filopodia number may represent an important effect of aggrecan molecules, as a "focusing" of growth cone connectivity through a reduction of "sensing" filopodia. Studies of hippocampal mossy fiber filopodia motility showed a similar phenomenon, in which filopodia motility was correlated with free extracellular space (Tashiro, et al., 2003). Therefore the aggrecan stripe represents a barrier, or reduction in free extracellular space, and is correlated with a reduction in filopodia number. Since this reduction is evident using CHO-745-derived aggrecan, it is likely a response to the presence of any variant of aggrecan (i.e., core protein), rather than a process of neurite inhibition. In contrast, following growth cone contact with COS-7 and BA I there was also a significant decrease in filopodia length. This result suggests that inhibition of outgrowing neurites by aggrecan at the point of the growth cone reduces the ability for the growth cone to "sense" its surroundings, as a reduction in filopodia length would limit filopodia contact with the surrounding environment. These results may represent the physical manifestation of aggrecan molecules orienting effect on neurites.

Inhibition following filopodia contact is associated with an increase in growth cone area

The CHO-K1 derived and A1A1D1-purified aggrecan (BA II) inhibited outgrowing neurites following filopodia contact with aggrecan. Inhibition at this level was associated with an increase in growth cone area. Similar to inhibition following growth cone contact, there were reductions in filopodia number and length following filopodia contact with BA II. These similar changes in filopodia behavior further support the "focusing" effect of aggrecan.

Filopodia contact with the aggrecan stripe caused a significant reduction in growth cone velocity

Growth cone velocity was significantly reduced following a single filopodia contact with BA I. This result was highly intriguing – that a single filopodial contact can induce a significant change in growth cone behavior. This result lies in parallel with our earlier

NIH-PA Author Manuscript

NIH-PA Author Manuscript

NIH-PA Author Manuscript

published results showing that CSPG-coated beads presented to a single filopodia induced a rapid increase in intracellular calcium leading to outgrowth inhibition (Snow, et al., 1994). BA I did not inhibit neurite outgrowth at the point of filopodia contact using this paradigm (although inhibition was the final result), the filopodial-induced reduction in velocity may represent another example of aggrecan-induced "focusing". Constructively, if slowed velocity is predictive of eventual inhibition, then perhaps agents that increase the rate of outgrowth following injury could improve the chances of growth cones to overcome inhibitory barriers, such as CSPGs. In fact there is some supporting evidence, for instance, neurons from younger animals grow much quicker and regenerate more effectively than older animals (Bernstein, 1964, Black and Lasek, 1979, Goldberg and Frank, 1981, Verdu, et al., 2000). In addition, an immunosuppressant drug (FK506) and cyclic-AMP are able to increase the rate of axonal growth, increase the overall rate of regeneration, and increase the amount of functional recovery (Gold, et al., 1995, Gold, et al., 1994, Neumann, et al., 2002, Qiu, et al., 2002). Whether or not the velocity of a growing neurite directly impacts its ability to grow across growth-inhibitory CSPGs is not known, but is a direction of interest to our laboratory.

Mechanism of aggrecan inhibition on an outgrowing neurite

The mechanism by which aggrecan, and CSPGs in general, inhibit neurite outgrowth is not fully understood. Evidence suggests that the protein tyrosine phosphatase, PTPσ, is activated upon binding of chondroitin sulfate and inhibits neurite outgrowth (Chien and Ryu, 2013, Coles, et al., 2011, Shen, et al., 2009). However, *in vivo*, enzymatic removal of either chondroitin sulfate or keratan sulfate chains enhances neurite outgrowth in models of spinal cord injury (SCI) (Bradbury, et al., 2002, Imagama, et al., 2011, Jefferson, et al., 2011). Since, PTPσ specifically binds chondroitin sulfate, the effect of keratan sulfate removal through the action of keratanase II suggests a separate receptor for keratan sulfate. In addition, chondroitin sulfate, keratan sulfate, and heparan sulfate chains may bind, block diffusion, or inhibit responsiveness of neurons to neurotrophic factors and cytokines. This further complicates the exact mechanism by which proteoglycans interact with an outgrowing neurite. For instance, treatment with BDNF, NGF, and NT-3 in combination with chondroitinase ABC promotes neurite growth *in vivo* (Garcia-Alias, et al., 2011, Massey, et al., 2008, Tropea, et al., 2003). There is also evidence that the responsive second messenger Rho kinase (Rock) is activated by the glycosaminoglycan side chains of aggrecan and inhibits the responsiveness of an outgrowing neurite to NGF and NT-3 (Chan, et al., 2008). Since most neurotrophic receptors belong to the class of tyrosine kinase receptors and are suggested to increase neurite outgrowth, there is likely an intricate interaction between kinase and phosphatase activity regulating the phosphorylation level of the outgrowing neurite, determining whether to stop or continue growing.

Aggrecan contains both keratan and chondroitin sulfate chains, and our structurally diverse aggrecan variants differ in the number and length of these chains, and likely contain fragments of the aggrecan core protein. This heterogeneity in purified aggrecan samples and the absence of a clear mechanism of action complicates the interpretation of our structurally diverse aggrecan variants and their effect on neurite outgrowth. However the absence of chondroitin sulfate chains on CHO-745-derived aggrecan permitted neurite outgrowth, further implying a role of chondroitin sulfate chains in neurite inhibition. The two aggrecan variants that permitted growth cone contact with the aggrecan stripe but subsequent inhibition (COS-7 and BA I) both contain chondroitin sulfate chains. Comparing the COS-7-derived aggrecan to that produced in CHO-K1 cells suggest that the number of chondroitin sulfate chains may be a contributing factor in the inhibition of an outgrowing neurite. CHO-K1-derived aggrecan contains a greater number of chondroitin sulfate chains comparatively to COS-7-derived aggrecan, and inhibited the outgrowing neurite at the point of filopodia

NIH-PA Author Manuscript

NIH-PA Author Manuscript

NIH-PA Author Manuscript

contact. Therefore it is possible, the greater the number of chondroitin sulfate chains the more NGF is bound, and the lack of NGF to bind the filopodia prevents growth of the neurite beyond that point. In contrast, the fewer chondroitin sulfate chains on COS-7-derived aggrecan, allows a greater amount of NGF stimulation, and allows growth of the growth cone up to the point of the aggrecan stripe, at which point a receptor (i.e. PTPσ) specifically on the growth cone that is not localized on the filopodia is activated causing inhibition. Indeed, NGF receptors are localized on both the growth cone and filopodia of an outgrowing neurite (Echarte, et al., 2007). Though the exact cellular localization of the PTPσ receptor is not known; future studies will address the localization and interaction of these putative receptors on an outgrowing neurite to understand the complex interaction of neurotrophic and inhibitory cues.

In the present study, we investigated two different preparations of bovine articular cartilage: a proprietary preparation (BA I) and one purified by our laboratory through the A1A1D1 method (BA II). Since the techniques used to purify these preparations of aggrecan relied on the chemical structure/interaction of aggrecan, not only full-length but fractions of the aggrecan molecules were present in the preparations. This is a limitation of the analytical techniques of aggrecan purification that is not easily overcome. Surprisingly, these two preparations caused different effects on outgrowing neurites, as BA I permitted the growth cone to contact the stripe, while BA II prevented growth cone contact (retraction) and inhibited outgrowth at the point of filopodia contact. These differences in response are likely due to different amounts and structure of aggrecan fragments present in each preparation, as BA I contained a greater amount of aggrecan fragments (data not shown). In addition, all aggrecan (full-length and fragments) present in the BA II preparation contained the G1 domain, which suggests that the G1 domain is highly inhibitory and prevents the growth cone from contacting the stripe. The presence of fragments is physiologically relevant as the extracellular matrix both normally and following injury contains a mixture of full-length and fragmented CSPGs, including aggrecan. The effect of these CSPG fragments is the focus of a separate study in our laboratory.

Conclusions

Aggrecan, and CSPGs, likely play a multipotent role in the injured spinal cord

Research suggests that targeting CSPGs to promote neuronal regeneration following SCI is a promising therapeutic approach. Enzymatic removal of chondroitin sulfate and keratan sulfate, cleavage of aggrecan, genetic knockout of CSPGs and enzymes necessary for chondroitin sulfate synthesis, all enhance neuronal regrowth following SCI in rodent models. Though extremely promising findings, regeneration of the injured spinal cord is a complex undertaking. Increasing the amount of neurite outgrowth through the injury site is a necessary step to reconnect the brain to areas caudal of the injury. However, once across the injury site a neurite needs to make the appropriate connection, and intact CSPGs may play a key role in this direction or “focusing”. The exact interaction and mechanisms by which CSPGs interact with an outgrowing neurite need to be determined in order to design the next generation of CSPG-oriented therapies. The results in this study suggest that structural variation in CSPGs determines the proximity of growth cone inhibition, possibly representing the interaction of various signaling pathways cueing the outgrowing neurite to either, grow, stop, or turn.

Acknowledgments

A preliminary report of these findings was presented at the annual meeting of the Blue Grass Chapter of the Society for Neuroscience, Lexington, KY. Support provided by the NIH (NINDS; NS053470); the Kentucky Spinal Cord and Head Injury Research Trust (#10-11A); and the Department of Defense (SC090248). Special acknowledgement

NIH-PA Author Manuscript

NIH-PA Author Manuscript

NIH-PA Author Manuscript

goes to the following undergraduate students, who, as part of their research experience (BIO-, ABT-, or CHEM-395), contributed to data collection and helpful discussions: Shawn Milburn, Matt Troese, Bailey Westerfield, and Brandon Sutton. The original Figure 1 illustration was created by Al Hering and edited further by Thomas Hering and Justin Beller.

Abbreviations

CSPG	Chondroitin Sulfate Proteoglycan
CHO	Chinese hamster ovary K1 (cell line)
COS7	Simian kidney cell line
BA	Bovine (Steer) articular cartilage aggrecan

References

Asher RA, Fidler PS, Rogers JH, Fawcett JW. TGF-ß stimulates neurocan synthesis in cultured rat astrocytes. Soc for Neurosci Abst. 1998; 24:56.

Asher RA, Morgenstern DA, Fidler PS, Adcock KH, Oohira A, Braistead JE, Levine JM, Margolis RU, Rogers JH, Fawcett JW. Neurocan is upregulated in injured brain and in cytokine-treated astrocytes. J Neurosci. 2000; 20:2427–2438. [PubMed: 10729323]

Barbosa I, Garcia S, Barbier-Chassefiere V, Caruelle JP, Martelly I, Papy-Garcia D. Improved and simple micro assay for sulfated glycosaminoglycans quantification in biological extracts and its use in skin and muscle tissue studies. Glycobiology. 2003; 13:647–653. [PubMed: 12773478]

Barritt AW, Davies M, Marchand F, Hartley R, Grist J, Yip P, McMahon SB, Bradbury EJ. Chondroitinase ABC promotes sprouting of intact and injured spinal systems after spinal cord injury. J Neurosci. 2006; 26:10856–10867. [PubMed: 17050723]

Beller JA, Gurkoff GG, Berman RF, Lyeth BG. Pharmacological enhancement of glutamate transport reduces excitotoxicity in vitro. Restor Neurol Neurosci. 2011; 29:331–346. [PubMed: 21846950]

Bernstein JJ. Relation of Spinal Cord Regeneration to Age in Adult Goldfish. Exp Neurol. 1964; 9:161–174. [PubMed: 14126124]

Black MM, Lasek RJ. Slowing of the rate of axonal regeneration during growth and maturation. Exp Neurol. 1979; 63:108–119. [PubMed: 467539]

Bradbury EJ, Moon LD, Popat RJ, King VR, Bennett GS, Patel PN, Fawcett JW, McMahon SB. Chondroitinase ABC promotes functional recovery after spinal cord injury. Nature. 2002; 416:636–640. [PubMed: 11948352]

Brown JM, Xia J, Zhuang B, Cho KS, Rogers CJ, Gama CI, Rawat M, Tully SE, Uetani N, Mason DE, Tremblay ML, Peters EC, Habuchi O, Chen DF, Hsieh-Wilson LC. A sulfated carbohydrate epitope inhibits axon regeneration after injury. Proc Natl Acad Sci U S A. 2012; 109:4768–4773. [PubMed: 22411830]

Busch SA, Silver J. The role of extracellular matrix in CNS regeneration. Curr Opin Neurobiol. 2007; 17:120–127. [PubMed: 17223033]

Chan CC, Roberts CR, Steeves JD, Tetzlaff W. Aggrecan components differentially modulate nerve growth factor-responsive and neurotrophin-3-responsive dorsal root ganglion neurite growth. J Neurosci Res. 2008; 86:581–592. [PubMed: 17918743]

Chien PN, Ryu SE. Protein tyrosine phosphatase sigma in proteoglycan-mediated neural regeneration regulation. Mol. Neurobiol. 2013; 47:220–227. [PubMed: 22956273]

Chierzi S, Ratto GM, Verma P, Fawcett JW. The ability of axons to regenerate their growth cones depends on axonal type and age, and is regulated by calcium, cAMP and ERK. Eur J Neurosci. 2005; 21:2051–2062. [PubMed: 15869501]

Coles CH, Shen Y, Tenney AP, Siebold C, Sutton GC, Lu W, Gallagher JT, Jones EY, Flanagan JG, Aricescu AR. Proteoglycan-specific molecular switch for RPTPsigma clustering and neuronal extension. Science. 2011; 332:484–488. [PubMed: 21454754]

NIH-PA Author Manuscript

NIH-PA Author Manuscript

NIH-PA Author Manuscript

Condic ML, Snow DM, Letourneau PC. Embryonic neurons adapt to the inhibitory proteoglycan aggrecan by increasing integrin expression. J Neurosci. 1999; 19:10036–10043. [PubMed: 10559411]

Davies S, Fitch M, Memberg S, Hall A, Raisman G, Silver J. Regeneration of adult axons in white matter tracts of the central nervous system. Nature. 1997; 390:680–683. [PubMed: 9414159]

Dityatev A, Schachner M, Sonderegger P. The dual role of the extracellular matrix in synaptic plasticity and homeostasis. Nat Rev Neurosci. 2010; 11:735–746. [PubMed: 20944663]

Echarte MM, Bruno L, Arndt-Jovin DJ, Jovin TM, Pietrasanta LI. Quantitative single particle tracking of NGF-receptor complexes: transport is bidirectional but biased by longer retrograde run lengths. FEBS Lett. 2007; 581:2905–2913. [PubMed: 17543952]

Esko JD, Stewart TE, Taylor WH. Animal cell mutants defective in glycosaminoglycan biosynthesis. Proc Natl Acad Sci U S A. 1985; 82:3197–3201. [PubMed: 3858816]

Faulkner JR, Herrmann JE, Woo MJ, Tansey KE, Doan NB, Sofroniew MV. Reactive astrocytes protect tissue and preserve function after spinal cord injury. J Neurosci. 2004; 24:2143–2155. [PubMed: 14999065]

Fitch MT, Silver J. Activated macrophages and the blood-brain barrier: inflammation after CNS injury leads to increases in putative inhibitory molecules. Exp. Neurol. 1997; 148:587–603. [PubMed: 9417835]

Fitch MT, Silver J. Glial cell extracellular matrix: boundaries for axon growth in development and regeneration. Cell Tissue Res. 1997; 290:379–384. [PubMed: 9321701]

Fok-Seang J, Smith-Thomas LC, Meiners S, Muir E, Du JS, Housden E, Johnson AR, Faissner A, Geller HM, Keynes RJ, et al. An analysis of astrocytic cell lines with different abilities to promote axon growth. Brain Res. 1995; 689:207–223. [PubMed: 7583324]

Frischknecht R, Seidenbecher CI. The crosstalk of hyaluronan-based extracellular matrix and synapses. Neuron Glia Biol. 2008; 4:249–257. [PubMed: 19811705]

Galtrey CM, Asher RA, Nothias F, Fawcett JW. Promoting plasticity in the spinal cord with chondroitinase improves functional recovery after peripheral nerve repair. Brain. 2007; 130:926–939. [PubMed: 17255150]

Garcia-Alias G, Barkhuysen S, Buckle M, Fawcett JW. Chondroitinase ABC treatment opens a window of opportunity for task-specific rehabilitation. Nat Neurosci. 2009; 12:1145–1151. [PubMed: 19668200]

Garcia-Alias G, Petrosyan HA, Schnell L, Horner PJ, Bowers WJ, Mendell LM, Fawcett JW, Arvanian VL. Chondroitinase ABC combined with neurotrophin NT-3 secretion and NR2D expression promotes axonal plasticity and functional recovery in rats with lateral hemisection of the spinal cord. J Neurosci. 2011; 31:17788–17799. [PubMed: 22159095]

Garwood J, Schnadelbach O, Clement A, Schutte K, Bach A, Faissner A. DSD-1-Proteoglycan is the mouse homolog of phosphacan and displays opposing effects on neurite outgrowth dependent on neuronal lineage. J. Neurosci. 1999; 19(10):3888–3899. [PubMed: 10234020]

Giuseppetti JM, McCarthy JB, Letourneau PC. Isolation and partial characterization of a cell-surface heparan sulfate proteoglycan from embryonic rat spinal cord. J. Neurosci. Res. 1994; 37:584–595. [PubMed: 8028039]

Gold BG, Storm-Dickerson T, Austin DR. The immunosuppressant FK506 increases functional recovery and nerve regeneration following peripheral nerve injury. Restor Neurol Neurosci. 1994; 6:287–296. [PubMed: 21551759]

Gold BG, Katoh K, Storm-Dickerson T. The immunosuppressant FK506 increases the rate of axonal regeneration in rat sciatic nerve. J Neurosci. 1995; 15:7509–7516. [PubMed: 7472502]

Goldberg S, Frank B. Do young axons regenerate better than old axons? Exp Neurol. 1981; 74:245–259. [PubMed: 7286119]

Gordon-Weeks PR. Growth at the growth cone. Trends Neurosci. 1989; 12:238–240. [PubMed: 2475932]

Horn KP, Busch SA, Hawthorne AL, van Rooijen N, Silver J. Another barrier to regeneration in the CNS: activated macrophages induce extensive retraction of dystrophic axons through direct physical interactions. J Neurosci. 2008; 28:9330–9341. [PubMed: 18799667]

NIH-PA Author Manuscript NIH-PA Author Manuscript NIH-PA Author Manuscript

Hynds DL, Snow DM. Fibronectin and laminin elicit differential behaviors from SH-SY5Y growth cones contacting inhibitory chondroitin sulfate proteoglycans. J Neurosci Res. 2001; 66:630–642. [PubMed: 11746383]

Iijima N, Oohira A, Mori T, Kitabatake K, Kohsaka S. Core protein of chondroitin sulfate proteoglycan promotes neurite outgrowth from cultured neocortical neurons. J. Neurochem. 1991; 56:706–708. [PubMed: 1988564]

Imagama S, Sakamoto K, Tauchi R, Shinjo R, Ohgomori T, Ito Z, Zhang H, Nishida Y, Asami N, Takeshita S, Sugiura N, Watanabe H, Yamashita T, Ishiguro N, Matsuyama Y, Kadomatsu K. Keratan sulfate restricts neural plasticity after spinal cord injury. J Neurosci. 2011; 31:17091–17102. [PubMed: 22114278]

Ivins JK, Parry MK, Long DA. A novel cAMP-dependent pathway activates neuronal integrin function in retinal neurons. J Neurosci. 2004; 24:1212–1216. [PubMed: 14762139]

Jefferson SC, Tester NJ, Howland DR. Chondroitinase ABC promotes recovery of adaptive limb movements and enhances axonal growth caudal to a spinal hemisection. J Neurosci. 2011; 31:5710–5720. [PubMed: 21490212]

Jones L, Margolis R, Tuszynski M. The chondroitin sulfate proteoglycans neurocan, brevican, phosphacan, and versican are differentially regulated following spinal cord injury. Experimental Neurology. 2003; 182:399–411. [PubMed: 12895450]

Juliano RL, Haskill S. Signal transduction from the extracellular matrix. J Cell Biol. 1993; 120:577–585. [PubMed: 8381117]

Klausmeyer A, Garwood J, Faissner A. Differential expression of phosphacan/RPTPbeta isoforms in the developing mouse visual system. J Comp Neurol. 2007; 504:659–679. [PubMed: 17722031]

Kofron CM, Fong VJ, Hoffman-Kim D. Neurite outgrowth at the interface of 2D and 3D growth environments. J Neural Eng. 2009; 6:016002. [PubMed: 19104140]

Koprivica V, Cho KS, Park JB, Yiu G, Atwal J, Gore B, Kim JA, Lin E, Tessier-Lavigne M, Chen DF, He Z. EGFR activation mediates inhibition of axon regeneration by myelin and chondroitin sulfate proteoglycans. Science. 2005; 310:106–110. [PubMed: 16210539]

Laabs TL, Wang H, Katagiri Y, McCann T, Fawcett JW, Geller HM. Inhibiting glycosaminoglycan chain polymerization decreases the inhibitory activity of astrocyte-derived chondroitin sulfate proteoglycans. J Neurosci. 2007; 27:14494–14501. [PubMed: 18160657]

Lemons M, Howland D, Anderson D. Chondroitin sulfate proteoglycan immunoreactivity increases following spinal cord injury and transplantation. Exp. Neurol. 1999; 160:51–65. [PubMed: 10630190]

Lemons ML, Barua S, Abanto ML, Halfter W, Condic ML. Adaptation of sensory neurons to hyalectin and decorin proteoglycans. J Neurosci. 2005; 25:4964–4973. [PubMed: 15901777]

Letourneau PC. Cell-to-substratum adhesion and guidance of axonal elongation. Devel. Biol. 1975; 44:92–101. [PubMed: 1132591]

Li GN, Liu J, Hoffman-Kim D. Multi-molecular gradients of permissive and inhibitory cues direct neurite outgrowth. Ann Biomed Eng. 2008; 36:889–904. [PubMed: 18392680]

Lorber B. Role of NG2 in Development and Regeneration. J. Neurosci. 2006; 26:7127–7128. [PubMed: 16826634]

Massey JM, Hubscher CH, Wagoner MR, Decker JA, Amps J, Silver J, Onifer SM. Chondroitinase ABC digestion of the perineuronal net promotes functional collateral sprouting in the cuneate nucleus after cervical spinal cord injury. J Neurosci. 2006; 26:4406–4414. [PubMed: 16624960]

Massey JM, Amps J, Viapiano MS, Matthews RT, Wagoner MR, Whitaker CM, Alilain W, Yonkof AL, Khalyfa A, Cooper NG, Silver J, Onifer SM. Increased chondroitin sulfate proteoglycan expression in denervated brainstem targets following spinal cord injury creates a barrier to axonal regeneration overcome by chondroitinase ABC and neurotrophin-3. Exp Neurol. 2008; 209:426–445. [PubMed: 17540369]

Masuda K, Shirota H, Thonar EJ. Quantification of 35S-labeled proteoglycans complexed to alcian blue by rapid filtration in multiwell plates. Anal Biochem. 1994; 217:167–175. [PubMed: 7515600]

NIH-PA Author Manuscript

NIH-PA Author Manuscript

NIH-PA Author Manuscript

Matthews RT, Kelly GM, Zerillo CA, Gray G, Tiemeyer M, Hockfield S. Aggrecan glycoforms contribute to the molecular heterogeneity of perineuronal nets. J Neurosci. 2002; 22:7536–7547. [PubMed: 12196577]

Maurel P, Rauch U, Flad M, Margolis RK, Margolis RU. Phosphacan, a chondroitin sulfate proteoglycan of brain that interacts with neurons and neural cell-adhesion molecules, is an extracellular variant of a receptor-type protein tyrosine phosphatase. Proc. Natl. Acad. Sci. USA. 1994; 91:2512–2516. [PubMed: 7511813]

McKeon R, Jurynec M, Buck C. The chondroitin sulfate proteoglycans neurocan and phosphacan are expressed by reactive astrocytes in the chronic CNS glial scar. J. Neurosci. 1999; 19:10778–10788. [PubMed: 10594061]

McKeon RJ, Hoke A, Silver J. Injury-induced proteoglycans inhibit the potential for laminin-mediated axon growth on astrocytic scars. Exp Neurol. 1995; 136:32–43. [PubMed: 7589332]

McKerracher L, Chamoux M, Arregui CO. Role of laminin and integrin interactions in growth cone guidance. Mol Neurobiol. 1996; 12:95–116. [PubMed: 8818145]

McRae PA, Rocco MM, Kelly G, Brumberg JC, Matthews RT. Sensory deprivation alters aggrecan and perineuronal net expression in the mouse barrel cortex. J Neurosci. 2007; 27:5405–5413. [PubMed: 17507562]

Miwa HE, Gerken TA, Huynh TD, Flory DM, Hering TM. Mammalian expression of full-length bovine aggrecan and link protein: formation of recombinant proteoglycan aggregates and analysis of proteolytic cleavage by ADAMTS-4 and MMP-13. Biochim Biophys Acta. 2006a; 1760:472–486. [PubMed: 16427204]

Miwa HE, Gerken TA, Hering TM. Effects of covalently attached chondroitin sulfate on aggrecan cleavage by ADAMTS-4 and MMP-13. Matrix Biol. 2006b; 25:534–545. [PubMed: 16945513]

Miwa HE, Gerken TA, Huynh TD, Duesler LR, Cotter M, Hering TM. Conserved sequence in the aggrecan interglobular domain modulates cleavage by ADAMTS-4 and ADAMTS-5. Biochim Biophys Acta. 2009; 1790:161–172. [PubMed: 19101611]

Moon LD, Asher RA, Rhodes KE, Fawcett JW. Relationship between sprouting axons, proteoglycans and glial cells following unilateral nigrostriatal axotomy in the adult rat. Neuroscience Research. 2002; 109:101–117.

Morawski M, Bruckner G, Jager C, Seeger G, Kunzle H, Arendt T. Aggrecan-based extracellular matrix shows unique cortical features and conserved subcortical principles of mammalian brain organization in the Madagascan lesser hedgehog tenrec (Echinops telfairi Martin, 1838). Neuroscience. 2010; 165:831–849. [PubMed: 19682554]

Myer D, Gurkoff G, Lee S, Hovda D, Sofroniew M. Essential protective roles of reactive astrocytes in traumatic brain injury. Brain. 2006; 129:2761–2772. [PubMed: 16825202]

Neumann S, Bradke F, Tessier-Lavigne M, Basbaum AI. Regeneration of sensory axons within the injured spinal cord induced by intraganglionic cAMP elevation. Neuron. 2002; 34:885–893. [PubMed: 12086637]

Nishiyama A, Dahlin KJ, Prince JT, Johnstone SR, Stallcup WB. The primary structure of NG2, a novel membrane-spanning proteoglycan. J. Cell Biol. 1991; 114:359–371. [PubMed: 1906475]

Oohira A, Matsui F, Watanabe E, Kushima Y, Maeda N. Developmentally regulated expression of a brain specific species of chondroitin sulfate proteoglycan, neurocan, identified with a monoclonal antibody 1G2 in the rat cerebrum. Neuroscience. 1994; 60:145–157. [PubMed: 8052408]

Pasterkamp R, Anderson P, Verhaagen J. Periheral nerve injury fails to induce growth of lesioned ascending dorsal column axons into spinal cord scar tissue expressing the axon repellent semaphorin3A. European Journal of Neuroscience. 2001; 13:457–471. [PubMed: 11168552]

Plant GW, Bates ML, Bunge MB. Inhibitory proteoglycan immunoreactivity is higher at the caudal than the rostral Schwann cell graft-transected spinal cord interface. Mol Cell Neurosci. 2001; 17:471–487. [PubMed: 11273643]

Qiu J, Cai D, Dai H, McAtee M, Hoffman PN, Bregman BS, Filbin MT. Spinal axon regeneration induced by elevation of cyclic AMP. Neuron. 2002; 34:895–903. [PubMed: 12086638]

Ramon y Cajal, S. Degenerationa and regeneration of the nervous system. Oxford University Press; London, Oxford UK: 1928.

NIH-PA Author Manuscript NIH-PA Author Manuscript NIH-PA Author Manuscript

Reichardt LF, Prokop A. Introduction: the role of extracellular matrix in nervous system development and maintenance. Dev Neurobiol. 2011; 71:883–888. [PubMed: 21898856]

Reimers S, Hartlage-Rubsamen M, Bruckner G, Rossner S. Formation of perineuronal nets in organotypic mouse brain slice cultures is independent of neuronal glutamatergic activity. Eur J Neurosci. 2007; 25:2640–2648. [PubMed: 17561838]

Ribotta M, Menet V, Privat A. Glial scar and axonal regeneration in the CNS: lessons from GFAP and vimentin transgenic mice. Acta Neurochir Suppl. 2004; 89:87–92. [PubMed: 15335106]

Schmidt CE, Dai J, Lauffenburger DA, Sheetz MP, Horwitz AF. Integrin-cytoskeletal interactions in neuronal growth cones. J Neurosci. 1995; 15:3400–3407. [PubMed: 7751919]

See J, Bonner J, Neuhuber B, Fischer I. Neurite outgrowth of neural progenitors in presence of inhibitory proteoglycans. J Neurotrauma. 2010; 27:951–957. [PubMed: 20102265]

Shen Y, Tenney AP, Busch SA, Horn KP, Cuascut FX, Liu K, He Z, Silver J, Flanagan JG. PTPsigma is a receptor for chondroitin sulfate proteoglycan, an inhibitor of neural regeneration. Science. 2009; 326:592–596. [PubMed: 19833921]

Silver J, Miller JH. Regeneration beyond the glial scar. Nat Rev Neurosci. 2004; 5:146–156. [PubMed: 14735117]

Simmons CA, Matlis S, Thornton AJ, Chen S, Wang CY, Mooney DJ. Cyclic strain enhances matrix mineralization by adult human mesenchymal stem cells via the extracellular signal-regulated kinase (ERK1/2) signaling pathway. J Biomech. 2003; 36:1087–1096. [PubMed: 12831733]

Smith GM, Strunz C. Growth factor and cytokine regulation of chondroitin sulfate proteoglycans by astrocytes. Glia. 2005; 52:209–218. [PubMed: 15968632]

Snow DM, Lemmon V, Carrino DA, Caplan AI, Silver J. Sulfated proteoglycans in astroglial barriers inhibit neurite outgrowth in vitro. Exp Neurol. 1990; 109:111–130. [PubMed: 2141574]

Snow DM, Lemmon V, Carrino DA, Caplan AI, Silver J. Sulfated proteoglycans in astroglial barriers inhibit neurite outgrowth in vitro. Exp Neurol. 1990a; 109:111–130. [PubMed: 2141574]

Snow DM, Steindler DA, Silver J. Molecular and cellular characterization of the glial roof plate of the spinal cord and optic tectum: a possible role for a proteoglycan in the development of an axon barrier. Dev Biol. 1990b; 138:359–376. [PubMed: 1690673]

Snow DM, Atkinson PB, Hassinger TD, Letourneau PC, Kater SB. Chondroitin sulfate proteoglycan elevates cytoplasmic calcium in DRG neurons. Dev Biol. 1994; 166:87–100. [PubMed: 7958462]

Snow DM, Brown EM, Letourneau PC. Growth cone behavior in the presence of soluble chondroitin sulfate proteoglycan (CSPG), compared to behavior on CSPG bound to laminin or fibronectin. Int J Dev Neurosci. 1996; 14:331–349. [PubMed: 8842808]

Snow DM, Mullins N, Hynds DL. Nervous system-derived chondroitin sulfate proteoglycans regulate growth cone morphology and inhibit neurite outgrowth: a light, epifluorescence, and electron microscopy study. Microsc Res Tech. 2001; 54:273–286. [PubMed: 11514984]

Song H, Ming G, He Z, Lehmann M, McKerracher L, Tessier-Lavigne M, Poo M. Conversion of neuronal growth cone responses from repulsion to attraction by cyclic nucleotides. Science. 1998; 281:1515–1518. [PubMed: 9727979]

Stichel CC, Niermann H, D'urso D, Lausberg F, Hermanns S, Muller HW. Basal membrane-depleted scar in lesioned CNS: characteristics and relationships with regenerating axons. Neurosci. 1999; 93:321–333.

Tashiro A, Dunaevsky A, Blazeski R, Mason CA, Yuste R. Bidirectional regulation of hippocampal mossy fiber filopodial motility by kainate receptors: a two-step model of synaptogenesis. Neuron. 2003; 38:773–784. [PubMed: 12797961]

Tom VJ, Steinmetz MP, Miller JH, Doller CM, Silver J. Studies on the development and behavior of the dystrophic growth cone, the hallmark of regeneration failure, in an in vitro model of the glial scar and after spinal cord injury. J Neurosci. 2004; 24:6531–6539. [PubMed: 15269264]

Tropea D, Caleo M, Maffei L. Synergistic effects of brain-derived neurotrophic factor and chondroitinase ABC on retinal fiber sprouting after denervation of the superior colliculus in adult rats. J Neurosci. 2003; 23:7034–7044. [PubMed: 12904464]

van den Hoogen BM, van Weeren PR, Lopes-Cardozo M, van Golde LM, Barneveld A, van de Lest CH. A microtiter plate assay for the determination of uronic acids. Anal Biochem. 1998; 257:107–111. [PubMed: 9514779]

NIH-PA Author Manuscript

NIH-PA Author Manuscript

NIH-PA Author Manuscript

Verdu E, Ceballos D, Vilches JJ, Navarro X. Influence of aging on peripheral nerve function and regeneration. J Peripher Nerv Syst. 2000; 5:191–208. [PubMed: 11151980]

Wang H, Katagiri Y, McCann TE, Unsworth E, Goldsmith P, Yu ZX, Tan F, Santiago L, Mills EM, Wang Y, Symes AJ, Geller HM. Chondroitin-4-sulfation negatively regulates axonal guidance and growth. J Cell Sci. 2008; 121:3083–3091. [PubMed: 18768934]

Yick LW, Cheung PT, So KF, Wu W. Axonal regeneration of Clarke's neurons beyond the spinal cord injury scar after treatment with chondroitinase ABC. Exp Neurol. 2003; 182:160–168. [PubMed: 12821386]

Yu X, Bellamkonda RV. Dorsal root ganglia neurite extension is inhibited by mechanical and chondroitin sulfate-rich interfaces. J Neurosci Res. 2001; 66:303–310. [PubMed: 11592128]

Zhou FQ, Walzer M, Wu YH, Zhou J, Dedhar S, Snider WD. Neurotrophins support regenerative axon assembly over CSPGs by an ECM-integrin-independent mechanism. J Cell Sci. 2006; 119:2787–2796. [PubMed: 16772333]

Zimmermann DR, Dours-Zimmermann MT. Extracellular matrix of the central nervous system: from neglect to challenge. Histochem Cell Biol. 2008; 130:635–653. [PubMed: 18696101]

Zuo J, Neubauer D, Dyess K, Ferguson TA, Muir D. Degradation of chondroitin sulfate proteoglycan enhances the neurite-promoting potential of spinal cord tissue. Exp Neurol. 1998a; 154:654–662. [PubMed: 9878200]

Zuo J, Ferguson TA, Hernandez YJ, Stetler-Stevenson WG, Muir D. Neuronal matrix metalloproteinase-2 degrades and inactivates a neurite-inhibiting chondroitin sulfate proteoglycan. J Neurosci. 1998b; 18:5203–5211. [PubMed: 9651203]

NIH-PA Author Manuscript

NIH-PA Author Manuscript

NIH-PA Author Manuscript

Highlights

- Structurally diverse aggrecan variants differentially inhibit neurite outgrowth
- Aggrecan variants cause different effects on growth cone and filipodia behavior
- Reduced filipodia number is a result of contact with a variety of aggrecan variants
- Neurite velocity is reduced following a single filipodia contact with aggrecan

NIH-PA Author Manuscript

NIH-PA Author Manuscript

NIH-PA Author Manuscript

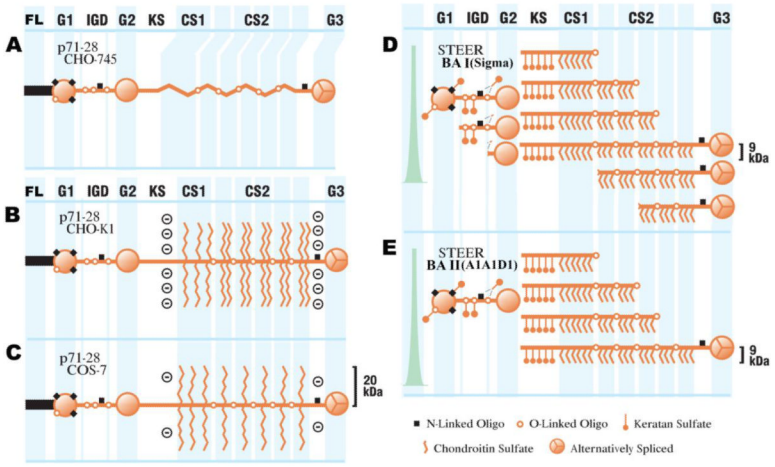

Figure 1. Structurally diverse aggrecan variants

Full-length aggrecan molecules contain 3 globular domains (G1, G2 and G3) connected by an interglobular domain (IGD; between G1 and G2) and a highly substituted stretch of amino acids, consisting of a domain of keratan sulfate substitution (KS) and two chondroitin sulfate substitution domains (CS1 and CS2) lying in between the G2 and G3 domain. In addition, the three recombinant aggrecan variants used in this study (CHO-745, CHO-K1, and COS-7) contain a FLAG peptide (FL). The appreciable differences in composition and content of the structurally diverse aggrecan variants are displayed. (A) CHO-745 aggrecan, (B) CHO-K1 aggrecan, (C) COS-7 aggrecan, (D) DEAE-purified steer bovine articular cartilage (BA I; Sigma), and (E) A1A1D1-purified steer bovine articular cartilage aggrecan (BA II). It is important to note the difference in fragmentation between BA I and BA II (D and E), as the A1A1D1-purified aggrecan contains only full-length protein or G1-containing fragments. For each of these variants the estimated chondroitin sulfate chain length is displayed in kDa. In addition, the degree of keratan sulfate and N-linked oligosaccharide substitution is also illustrated.

NIH-PA Author Manuscript

NIH-PA Author Manuscript

NIH-PA Author Manuscript

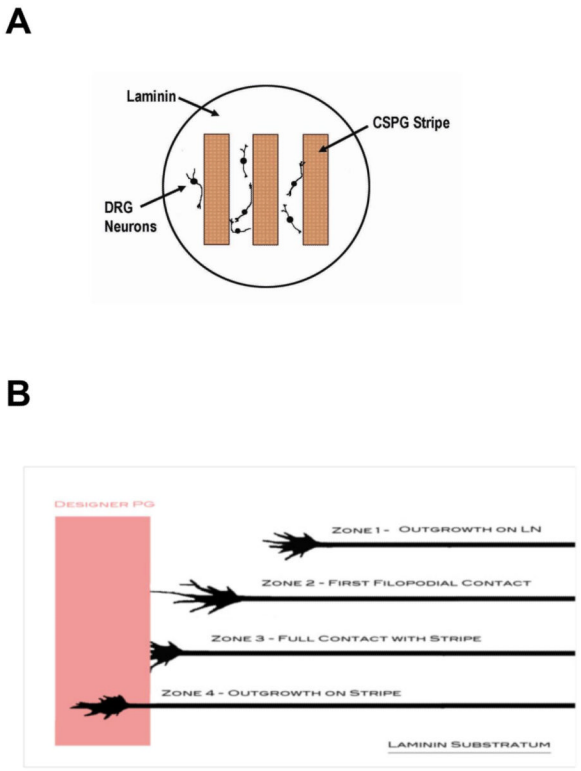

Figure 2. A schematic diagram of the tissue culture paradigm for testing dorsal root ganglion (DRG) neuron responses to substratum-bound aggrecan

(A) The tissue culture substratum was coated with poly-D-lysine (0.1 mg/ml) to bind protein. Aggrecan (150 μg/ml) was adsorbed in a stripe pattern. Laminin (25 μg/ml) was coated over the entire dish to create alternating lanes of laminin and aggrecan/laminin. (Adsorption of each aggrecan variant was done using the same technique and concentration, but in different cultures dishes for each; 3 replicates each). DRG neurons (E9–12) were seeded over the entire dish, and bound to laminin-only regions of the dish. (B) Time-lapse video-microscopy was used to observe outgrowth behaviors on laminin and as neurons encountered aggrecan/laminin-adsorbed regions. For analyses, examination points consisted of 1) outgrowth on laminin alone (Zone 1); 2) the point at which the first filopodia contacted the aggrecan-adsorbed area (Zone 2); 3) the transition zone when the growth cone was fully in contact with the aggrecan-adsorbed stripe (Zone 3); 4) outgrowth onto the aggrecan stripe (Zone 4; not used in analysis).

NIH-PA Author Manuscript

NIH-PA Author Manuscript

NIH-PA Author Manuscript

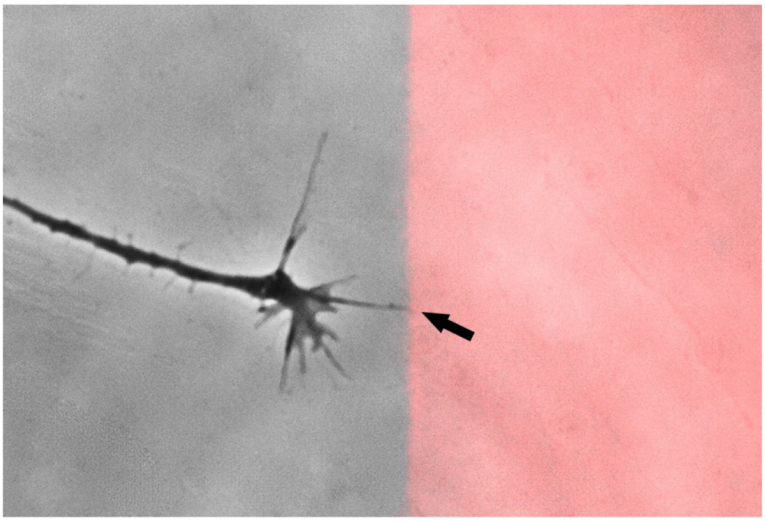

Figure 3. First filopodial contact

Growth cones elongate rapidly and efficiently on laminin alone (left side of image). As they elongate, they send out filopodia that sample the substratum, e.g. aggrecan labeled with Alexa 555 (right side of image; red). Changes in growth cones and filopodia can subsequently be observed following the initial filopodial contact with aggrecan (tip of arrow).

NIH-PA Author Manuscript

NIH-PA Author Manuscript

NIH-PA Author Manuscript

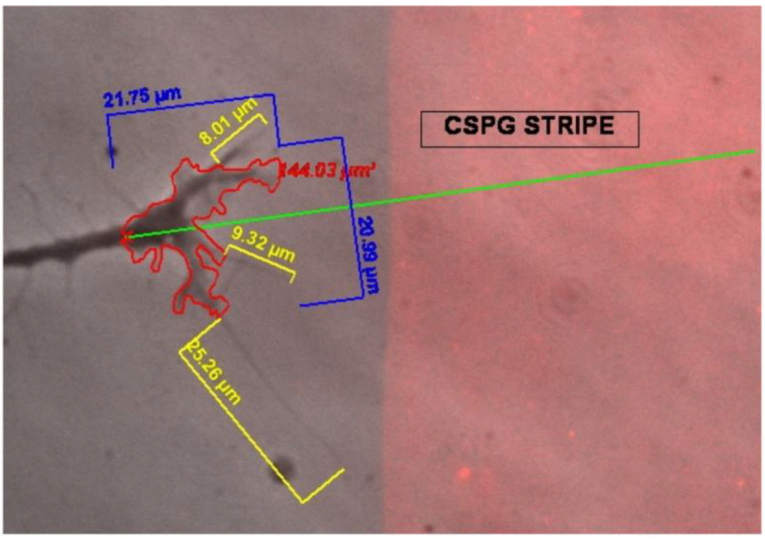

Figure 4. Annotation and growth cone analyses from time-lapse images

For each growth cone meeting the screening criteria, analyses were made of a wide variety of growth cone behaviors. Using specific tools provided by the Zeiss Axiovision system (Version 4.4), annotations were made on the images to perform measurements, e.g. growth cone width and length (blue), growth cone total area (red; excluding filopodia), filopodial length and number (yellow), and growth cone vector and angle of approach (green). A representative image with annotated measurements is shown here.

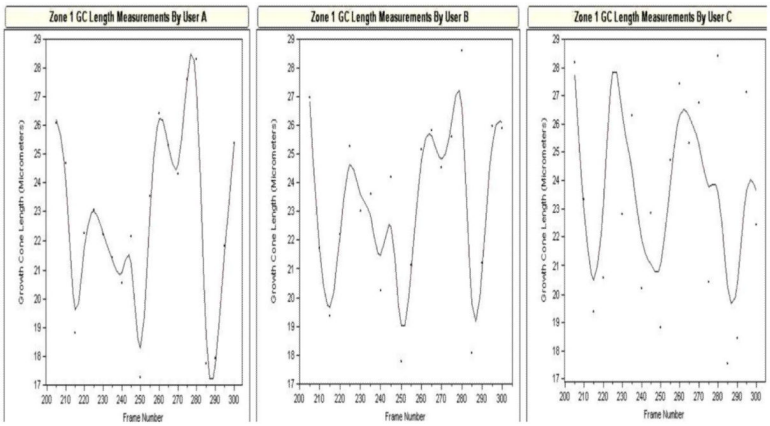

Figure 5. User consistency

The value of the data analyzing subtle and specific growth cone behaviors depends highly on consistency and accuracy by those doing the measurements. The left two panels represent data collected from two experimenters (Users A and B) who were trained, experienced at these types of measurements, and followed a conservative, detailed rubric for measurement, in this case, of growth cone length. The right panel (User C) represents data collected by a novice experimenter, who followed the rubric precisely. Although not as alike as A and B, user C clearly measures consistent trends, showing the value of the detailed rubric. Only data collected by trained, experienced experimenters (>20 traces) who precisely followed the rubric were used for this report.

NIH-PA Author Manuscript NIH-PA Author Manuscript NIH-PA Author Manuscript

NIH-PA Author Manuscript
NIH-PA Author Manuscript
NIH-PA Author Manuscript

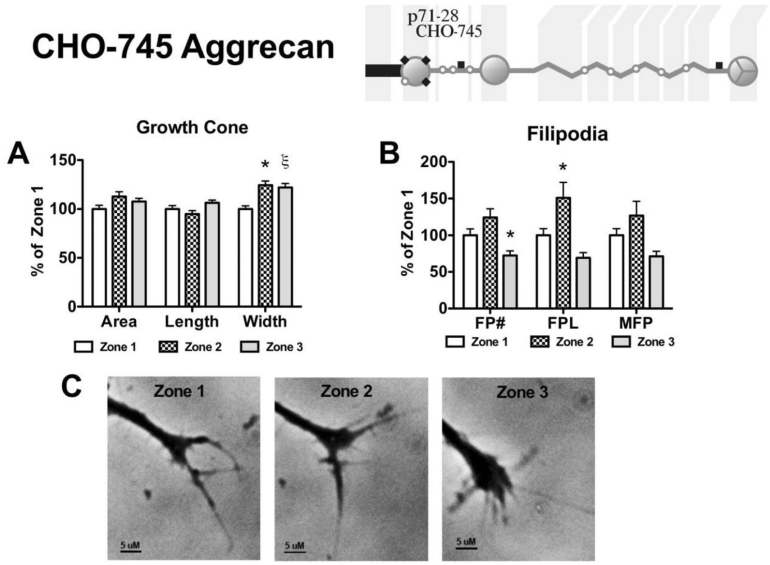

Figure 6. Effects on growth cone and filopodia behavior following contact with CHO-745 derived aggrecan

Aggrecan (150 μg/mL) derived from CHO-745 cells was placed on a laminin-coated glass coverslip in a stripe to determine the effect contact with the aggrecan has on an elongating neurite. (Insert) CHO-745 derived aggrecan contains no chondroitin sulfate substitutions. (A) Effect of filopodial (Zone 2) and growth cone (Zone 3) contact on growth cone area, growth cone length, growth cone width, and (B) filopodia behavior; FP#, number of filopodia; FPL, total filopodial length; MFP, max filopodial length. (C) Representative phase-contrast micrographs of an individual growth cone in the 3 different zones, scale bar = 5 μM. *, $p<0.05$; ξ, $p<0.001$, n=3.

NIH-PA Author Manuscript

NIH-PA Author Manuscript

NIH-PA Author Manuscript

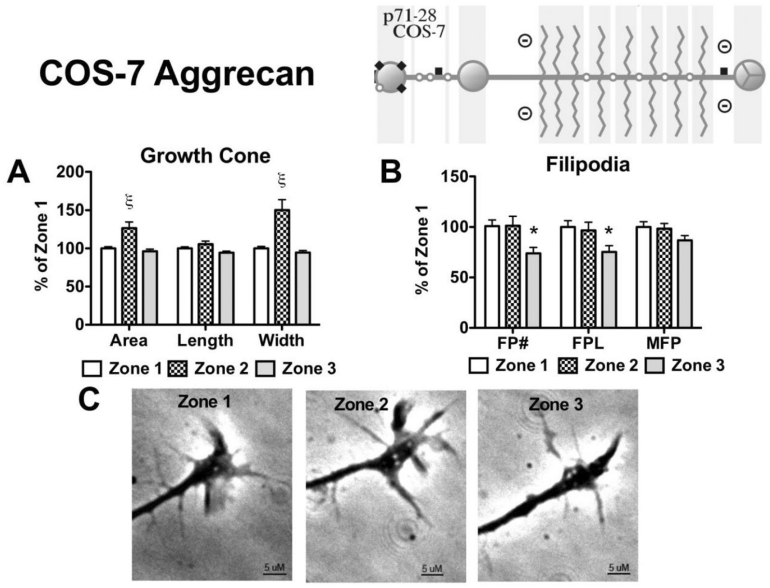

Figure 7. Effects on growth cone and filopodia behavior following contact with COS-7 derived aggrecan

Aggrecan (150 μg/mL) derived from COS-7 cells was placed on a laminin-coated glass coverslip in a stripe to determine the effect contact with the aggrecan has on an elongating neurite. (Insert) COS-7 derived aggrecan contains sparse chondroitin sulfate substitutions, with approximate chain length of 20 kDa. (A) Effect of filopodial (Zone 2) and growth cone (Zone 3) contact on growth cone area, growth cone length, growth cone width, and (B) filopodia behavior; FP#, number of filopodia; FPL, total filopodial length; MFP, max filopodial length. (C) Representative phase-contrast micrographs of an individual growth cone in the 3 different zones, scale bar = 5 μM. *, $p<0.05$; ξ , $p<0.001$, n=3.

NIH-PA Author Manuscript

NIH-PA Author Manuscript

NIH-PA Author Manuscript

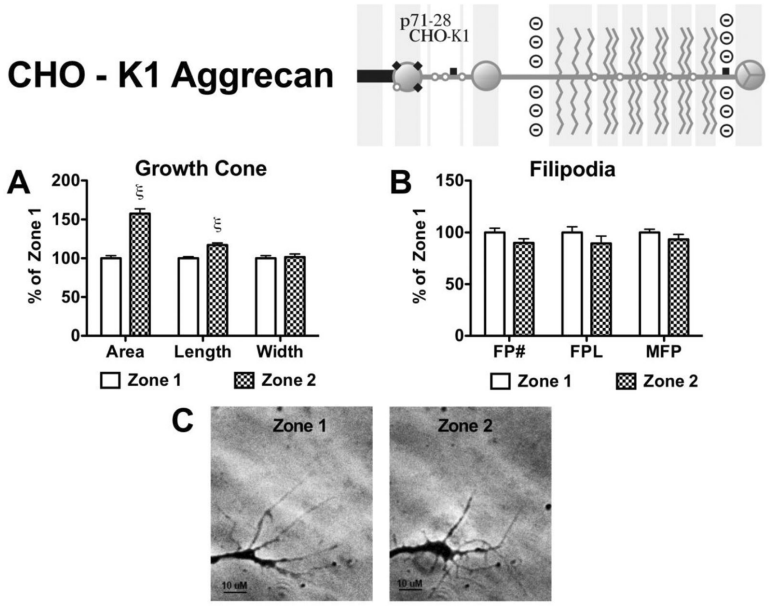

Figure 8. Effects on growth cone and filopodia behavior following contact with CHO-K1 derived aggrecan

Aggrecan (150 μg/mL) derived from CHO-K1 cells was placed on a laminin-coated glass coverslip in a striped pattern to determine the effect contact with the aggrecan has on an elongating neurite. (Insert) CHO-K1 derived aggrecan contains tightly packed chondroitin sulfate substitutions, with approximate chain length of 20 kDa. (A) Effect of filopodial (Zone 2) contact on growth cone area, growth cone length, growth cone width, and (B) filopodia behavior; FP#, number of filopodia; FPL, total filopodial length; MFP, max filopodial length. (C) Representative phase-contrast micrographs of an individual growth cone in the 2 different zones, scale bar = 10 μM. *, $p<0.05$; ξ, $p<0.001$, n=3.

NIH-PA Author Manuscript

NIH-PA Author Manuscript

NIH-PA Author Manuscript

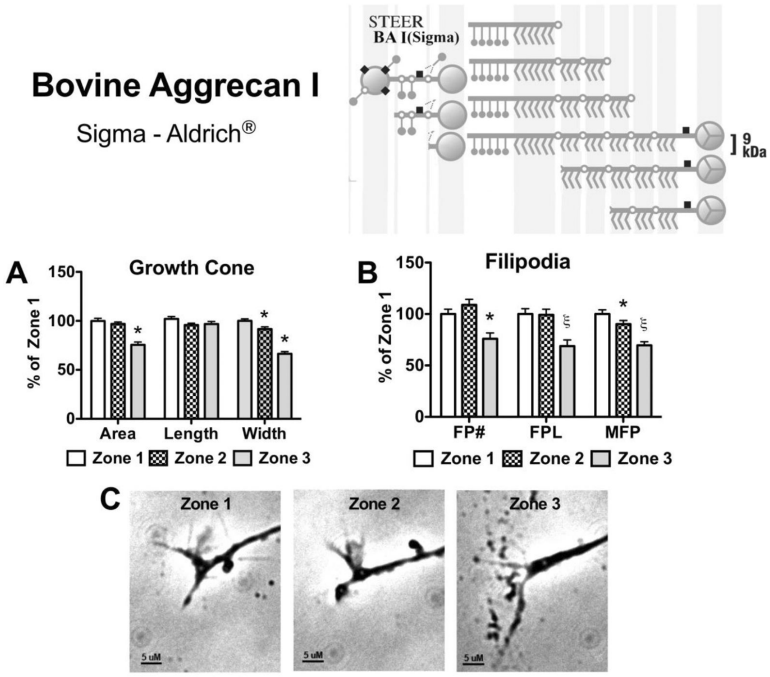

Figure 9. Effects on growth cone and filopodia behavior following contact with bovine articular cartilage derived aggrecan type I

Aggrecan (150 μg/mL) derived from bovine articular cartilage through DEAE chromatography (Sigma-Aldrich; BA I) was placed on a laminin-coated glass coverslip in a stripe to determine the effect contact with the aggrecan has on an elongating neurite. (Insert) BA I aggrecan contains very dense chondroitin sulfate substitutions with approximate chain length of 9 kDa, and fragments cleaved from both the N- and C-terminus. (A) Effect of filopodial (Zone 2) and growth cone (Zone 3) contact on growth cone area, growth cone length, growth cone width, and (B) filopodia behavior; FP#, number of filopodia; FPL, total filopodial length; MFP, max filopodial length. (C) Representative phase-contrast micrographs of an individual growth cone in the 3 different zones. Note beading and growth cone retraction in micrograph of Zone 3, scale bar = 5 μM. *, $p<0.05$; ξ, $p<0.001$, n=3.

NIH-PA Author Manuscript

NIH-PA Author Manuscript

NIH-PA Author Manuscript

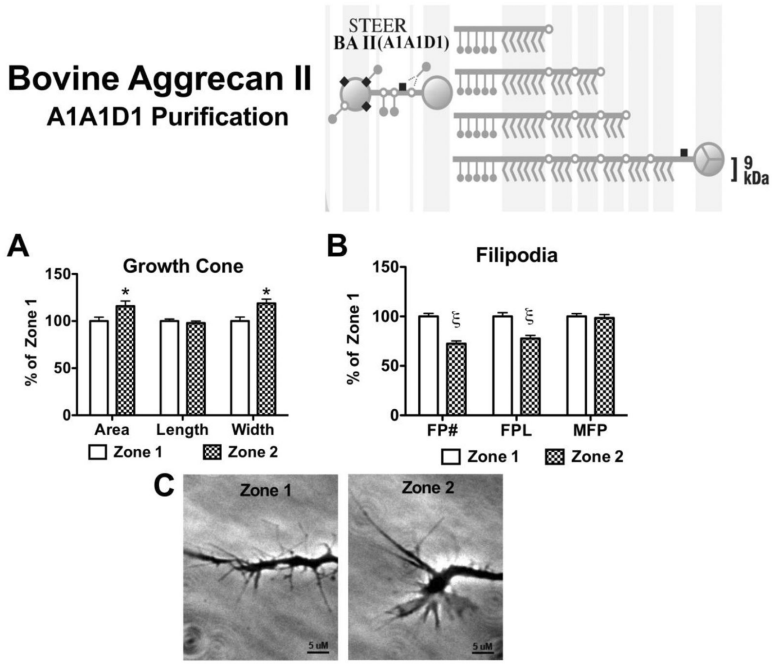

Figure 10. Effects on growth cone and filopodia behavior following contact with bovine articular cartilage derived aggrecan type II

Aggrecan (150 μg/mL) derived from bovine articular cartilage through A1A1D1 purification was placed on a laminin-coated glass coverslip in a striped pattern to determine the effect contact with the aggrecan has on an elongating neurite. (Insert) BA II aggrecan contains very dense chondroitin sulfate substitutions with approximate chain length of 9 kDa. All aggrecan molecules in this preparation contain the G1 domain. BA II prevented neurite outgrowth into Zone 3. (A) Effect of filopodial (Zone 2) contact on growth cone area, growth cone length, growth cone width, and (B) filopodia behavior; FP#, number of filopodia; FPL, total filopodial length; MFP, max filopodial length. (C) Representative phase-contrast micrographs of an individual growth cone in the 2 different zones, scale bar = 5 μM. *, $p<0.05$; ξ, $p<0.001$, n=3.

NIH-PA Author Manuscript

NIH-PA Author Manuscript

NIH-PA Author Manuscript

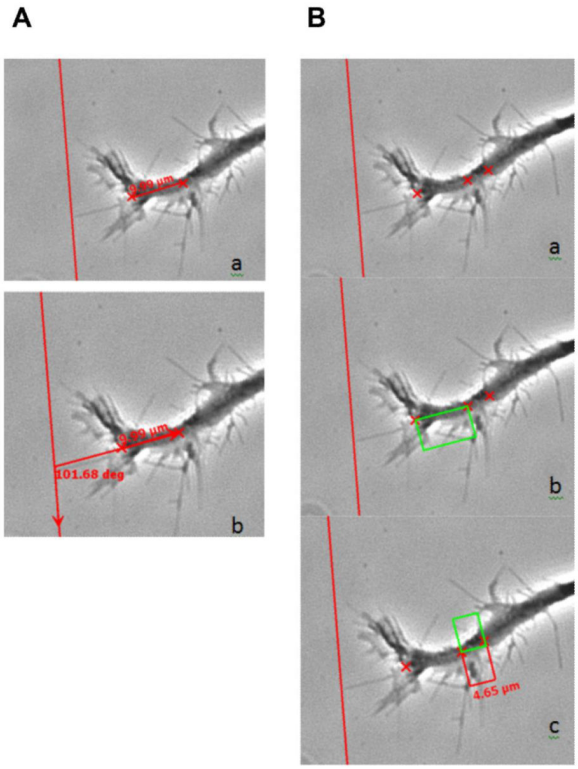

Figure 11. Method of analyzing the approach angle and growth cone velocity

A) Phase contrast images of a growth cone approaching the CSPG-adsorbed stripe. The left-most X marks the end of the growth cone central domain and the right X marks the growth cone root (panel a; see Methods); b) When extended to the CSPG border (red vertical line), the growth cone angle of approach can be determined by comparing to a line parallel to the CSPG border. B) The left-most and middle X's (panels a and b) are the same as in Figure 8, in that they mark the end of the growth cone central domain and growth cone root, respectively. The right-most X is the position of the growth cone root of a frame that is ten frames prior to the one shown. That is, the change in growth cone root position over time approximates a velocity for the frame. b) A drawn parrallelogram assists in c) measuring distance (change in growth cone root position).

NIH-PA Author Manuscript

NIH-PA Author Manuscript

NIH-PA Author Manuscript

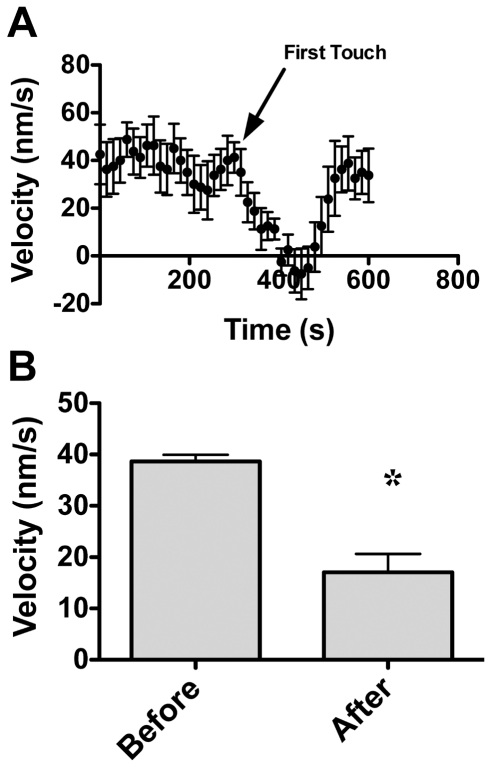

Figure 12. Growth cone velocity changes with single filopodial contact

(A) The velocity of an outgrowing neurites growth cone was measured for 20 frames prior to filopodia contact and 20 frames following filopodia contact. (A) Growth cone velocity versus time. The arrow indicates the point of first filopodial contact (n=8; time lapse series of one growth cone from each of 8 different animals). (B) Velocity before and after contact were averaged for direct comparison (n=8; * is $p<0.001$).

NIH-PA Author Manuscript
NIH-PA Author Manuscript
NIH-PA Author Manuscript

Table 1

Summary of Behavioral Analysis Values expressed as percent change from Zone 1.

	Zone 2						Zone 3						
	Area	**Length**	**Width**	**Filipodia Number**	**Filipodia Length**	**Max Filipodia Length**	**Area**	**Length**	**Width**	**Filipodia Number**	**Filipodia Length**	**Max Filipodia Length**	**Growth Across Stripe**
CHO-745	------	+12.7%	------	------	+50.9%	------	+7.6%	------	+21.9%	−27.6%	------	------	Yes
COS-7	+26.5%		+50.3%	------	------	------	------	------	------	−26.1%	−24.7%	------	No
CHO-K1	+57.6%	+17%	------	------	------	------							No
BAI	------	------	−7.3%	------	------	------	−24.4%	------	−33.6%	−24.1%	−31.2%	−30.4%	No
BAII	+15.9%	------	------	−27.5%	−22.3%	------							No